AD-A076 027 CALIFORNIA INST OF TECH PASADENA DIV OF ENGINEERING--ETC F/G 20/11
ANTI-PLANE SHEAR FIELDS WITH DISCONTINUOUS DEFORMATION GRADIENT--ETC(U)
SEP 79 J K KNOWLES , E STERNBERG N00014-75-C-0196

UNCLASSIFIED NL

| OF |
AD
A076027

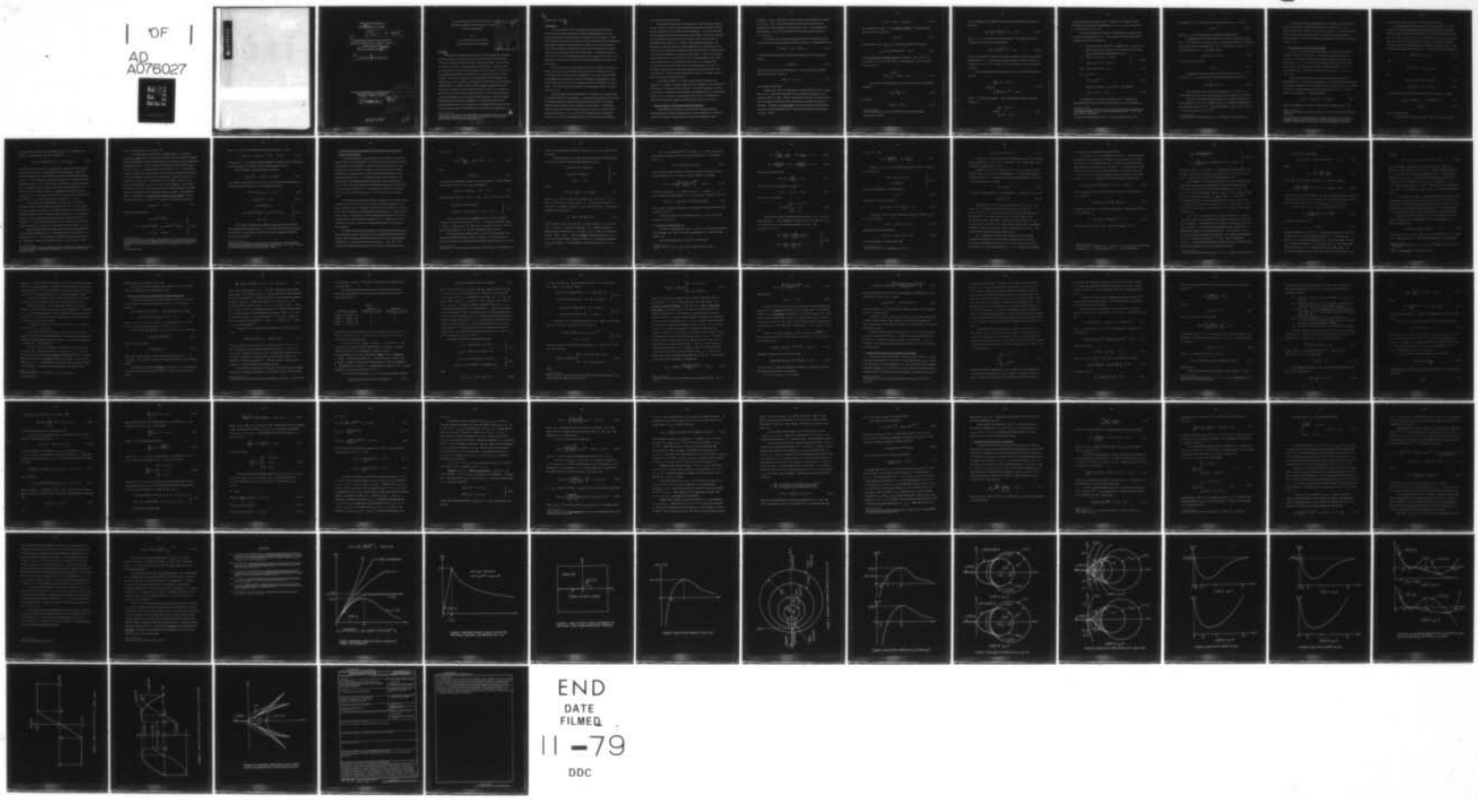

END
DATE
FILMED
11-79
DDC

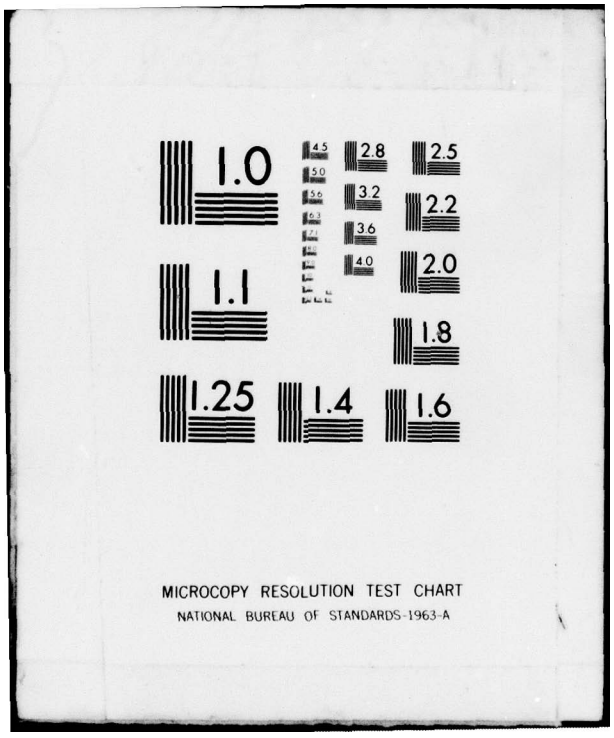
1.0
1.1
1.25
1.4
1.6
1.8
2.0
2.2
2.5
2.8
3.2
3.6
4.0
4.5
5.0
5.6
MICROCOPY RESOLUTION TEST CHART
NATIONAL BUREAU OF STANDARDS-1963-A

Office of Naval Research
(15) Contract N00014-75-C-0196
(9) Research Rept.,

(6) Anti-plane shear fields with discontinuous deformation gradients near the tip of a crack in finite elastostatics.

(14) TR-
Technical Report No. 43

(10) by
J. K. Knowles and Eli Sternberg

Division of Engineering and Applied Science
California Institute of Technology
Pasadena, California 91125

(11) September, 1979
(12) 71

Anti-plane shear fields with discontinuous deformation gradients near the tip of a crack in finite elastostatics*

by

J. K. Knowles and Eli Sternberg

California Institute of Technology

Summary

This paper reconsiders the problem of determining the elastostatic field near the tip of a crack in an all-around infinite body deformed by a "Mode III" loading at infinity to a state of anti-plane shear. The problem is treated for a class of incompressible, homogeneous, isotropic elastic materials whose constitutive laws permit a loss of ellipticity in the governing displacement equation of equilibrium at sufficiently severe shearing strains. The analysis represents a generalization of that reported in an earlier study and, as before, is carried out for the "small-scale nonlinear crack problem", in which a crack of finite length is replaced by a semi-infinite one, and the nonlinear field far from the crack-tip is matched to the near field predicted by the linearized theory. The methods employed in the present paper are necessarily largely qualitative, since they apply to all materials in the class considered. The principal feature of the resulting elastic field is the presence of two symmetrically located curves issuing from the crack-tip and bearing discontinuities in displacement

*The results communicated in this paper were obtained in the course of an investigation supported in part by Contract N00014-75-C-0196 with the Office of Naval Research in Washington, D. C.

gradient and stress.

Introduction

In a recent paper [1] we investigated the elastostatic field near the tip of a crack under conditions of finite anti-plane shear for a very special hypothetical incompressible – homogeneous and isotropic – elastic material whose constitutive law permits a loss of ellipticity of the appropriate displacement equation of equilibrium at sufficiently severe deformations. The problem treated in [1] involves an all-around infinite body containing a plane crack of constant width and infinite length. At infinity the body is subjected to a state of simple shear parallel to the edges of the crack. The analysis reported in [1] is carried out within the framework of finite elasticity theory.

When the amount of shear applied at infinity is small, the field near either crack-tip can be determined on the basis of an asymptotic scheme in which the crack of finite width is replaced by one of semi-infinite width, and the far field is required to match the elastostatic field near the crack-tip predicted by the solution to the original problem according to the linear theory. It is this "small-scale nonlinear crack problem" which is studied in detail in [1].

The particular material considered in [1] belongs to a special class of incompressible elastic materials. A characterizing property of this class is that each material in it has a strain energy density that is completely determined by the shear stress response in simple shear. The specific member of this class used in the pilot example of [1] was chosen with two requirements in mind: it was to allow for a potential loss of ellipticity, and it was to permit a fully explicit solution of the small-scale nonlinear

crack problem described above.

The anti-plane shear field near the tip of a crack had been analyzed earlier in [2] for a class of incompressible elastic materials which remain elliptic regardless of the severity of the deformation. For such materials, the elastostatic field is infinitely smooth in the interior of the body, although the displacement gradients as well as at least some of the stresses are unbounded at the crack-tip. In contrast, the example discussed in [1] shows that a material capable of losing ellipticity will in general give rise to a field near a crack-tip in which even the first derivatives of displacement are no longer continuous everywhere in the interior. In fact, the principal distinguishing feature of the results in [1] is the appearance in the elastostatic field of two curves, issuing from the crack-tip, symmetrically located with respect to the crack-axis, and terminating in the interior of the body, across which stresses and displacement gradients suffer jump discontinuities. Some of the local properties of such "elastostatic shocks" have been discussed elsewhere [3,4].

In the present paper, we treat the small-scale nonlinear crack problem for a <u>class</u> of incompressible materials capable of losing ellipticity – rather than for a single specific material. Although the analysis is based, as in [1], on a hodograph transformation, the emphasis here is on qualitative results and, in contrast to the arguments used in [1], the methods employed do not depend on explicit solvability of the equations involved.

1. <u>Special classes of incompressible elastic materials</u>

A homogeneous, isotropic, incompressible elastic material is characterized by a strain energy density (or elastic potential) W which is in general a function of the first two of the three fundamental scalar

invariants I_1, I_2, I_3 of the left (or right) Cauchy-Green deformation tensor: $W = W(I_1, I_2)$. Since only locally volume-preserving deformations are admissible for such materials, one always has $I_3 = 1$. In the undeformed configuration, $I_1 = I_2 = 3$; in any locally volume-preserving deformation, $I_1 \geq 3$ and $I_2 \geq 3$.

The special class of incompressible materials with which we shall be exclusively concerned consists of those for which W is independent of I_2:

$$W = W(I_1) \quad , \quad I_1 \geq 3 \quad ; \quad W(3) = 0 \quad . \tag{1.1}$$

At infinitesimal deformations, the shear modulus for such a material is given by

$$\mu = 2W'(3) > 0 \quad , \tag{1.2}$$

where the prime indicates differentiation. One can show that the Baker-Ericksen inequality reduces to

$$W'(I_1) > 0 \quad \text{for} \quad I_1 > 3 \tag{1.3}$$

for materials of this kind.

Suppose that a body is composed of a material with the strain energy density (1.1), and assume that the region occupied by the body in its undeformed state is a cube. Choose a rectangular cartesian coordinate frame with its origin at one vertex of the cube and axes collinear with three of the edges. Consider the <u>simple shear</u> in which a particle with coordinates x_1, x_2, x_3 in the undeformed state is carried to the point with coordinates y_1, y_2, y_3, where

$$y_1 = x_1 \ , \quad y_2 = x_2 \ , \quad y_3 = x_3 + kx_2 \ ; \tag{1.4}$$

the nonnegative constant k is the amount of shear.[1] In simple shear[2] the invariant I_1 is given by

$$I_1 = 3 + k^2 \ , \tag{1.5}$$

and the shear stress $\tau_{32} = \tau_{23}$ is related to the amount of shear by

$$\tau_{32} = \tau_{23} = \tau(k) \equiv 2kW'(3 + k^2) \ , \quad k \geq 0 \ . \tag{1.6}$$

The response curve in simple shear is the graph of $\tau(k)$. From (1.1), (1.5) and (1.6) it is clear that $W(I_1)$ is determined by $\tau(k)$ according to the formula

$$W(I_1) = \int_0^{\sqrt{I_1 - 3}} \tau(k)dk \ , \quad I_1 \geq 3 \ . \tag{1.7}$$

The simplest case for which (1.1) holds is that of the Neo-Hookean material:

$$W(I_1) = \frac{\mu}{2}(I_1 - 3) \ , \tag{1.8}$$

for which

$$\tau(k) = \mu k \ , \quad k \geq 0 \ . \tag{1.9}$$

---

[1] The deformation (1.4) is of course locally volume-preserving.

[2] See Section 2 of [2].

A second example is furnished by the "power-law materials" introduced in [2]; here

$$W(I_1) = \frac{\mu}{2b}\left\{\left[1 + \frac{b}{n}(I_1 - 3)\right]^{n} - 1\right\} \quad , \quad I_1 \geq 3 \quad , \tag{1.10}$$

where μ, n, b are positive material constants. The response curve in simple shear in this case is described by

$$\tau(k) = \mu\left(1 + \frac{b}{n}k^2\right)^{n-1} k \quad , \quad k \geq 0 \quad . \tag{1.11}$$

Figure 1 illustrates the response in shear for various values of the "hardening parameter" n. A power-law material hardens or softens in shear according as $n > 1$ or $n < 1$. The case $n = 1$ corresponds to the Neo-Hookean material.

The special material considered in [1] has a strain energy density given by

$$W(I_1) = \begin{cases} \frac{\mu}{2}(I_1 - 3) \quad , \quad 3 \leq I_1 \leq 4 \quad , \\ \\ -\frac{3\mu}{2} + 2\mu(I_1 - 3)^{1/4} \quad , \quad I_1 \geq 4 \quad , \end{cases} \tag{1.12}$$

where μ is a positive constant. The corresponding response in simple shear is:

$$\tau(k) = \begin{cases} \mu k \quad , \quad 0 \leq k \leq 1 \quad , \\ \\ \mu k^{-1/2} \quad , \quad k \geq 1 \quad . \end{cases} \tag{1.13}$$

Figure 2 displays the graph of (1.13). Note that $\tau'(k)$ suffers a jump discontinuity at the peak corresponding to $k=1$ (or $I_1=4$), and observe as well that $\tau(k)\to 0$ as $k\to\infty$.

In the present paper we shall be concerned with a subclass of the materials characterized by (1.1). This subclass contains all materials satisfying the following conditions:

(i) The strain energy density W satisfies (1.1), (1.2) and (1.3), and the shear-stress response $\tau(k)$ given by (1.6) is three times continuously differentiable for $k\geq 0$.

(ii) $$\left.\begin{aligned} &\tau'(k)>0 \text{ for } 0\leq k<1 \ , \ \tau'(1)=0 \ , \\ &\tau'(k)<0 \text{ for } k>1 \ , \ \tau''(1)<0 \ . \end{aligned}\right\} \qquad (1.14)^1$$

(iii) $$-\tau(k)<k\tau'(k)<\tau(k) \ , \quad k>0 \ . \qquad (1.15)$$

(iv) As $k\to\infty$,

$$\tau(k)\sim\tau_\infty+hk^{-1+\epsilon} \ , \qquad (1.16)$$

where the constants τ_∞, h and ϵ are such that

$$\tau_\infty\geq 0 \ , \ h>0 \ , \ 0<\epsilon<1 \ . \qquad (1.17)^2$$

According to (i), we have $\tau(k)\sim\mu k$ as $k\to 0$. Condition (ii) asserts that the response curve in simple shear rises monotonically to

---

[1] Condition (i) and the first three of the four requirements in condition (ii) automatically imply $\tau''(1)\leq 0$. We exclude the possibility $\tau''(1)=0$ only for reasons of simplicity.

[2] It may be confirmed that (1.16), (1.17) are consistent with (1.15).

a maximum[1] at $k = 1$, then declines to the limiting value τ_∞. We set

$$\tau_m = \tau(1) \ ; \tag{1.18}$$

evidently τ_m is the maximum stress attained in simple shear.

The right half of the double inequality in condition (iii) holds trivially for $k \geq 1$ by condition (ii), but for $k < 1$ it represents an additional restriction and asserts that the "shear modulus" $\tau(k)/k$ at an amount of shear k is a decreasing function of k. This implies that

$$\tau_m k \leq \tau(k) \leq \mu k \ , \quad 0 \leq k \leq 1 \ , \tag{1.19}$$

which in turn requires that

$$\mu \geq \tau_m \ . \tag{1.20}$$

The left half of the inequality (1.15) follows from (1.14) for $0 < k \leq 1$, but not for $k > 1$. It requires that $k\tau(k)$ be increasing and hence that

$$\tau(k) > \frac{\tau_m}{k} \text{ for } k > 1 \ . \tag{1.21}$$

Finally condition (iv) permits the limiting value of $\tau(k)$ as $k \to \infty$ to be either positive or zero and restricts the rate of approach to this limit.

The power-law materials described by (1.11) satisfy conditions (i)-(iv) provided $0 < n < 1/2$, if one takes $b = n/1 - 2n$, so that the maximum in the response curve is at $k = 1$. In this case one has $\tau_\infty = 0$, $h = \mu(1 - 2n)^{1-n}$, $\epsilon = 2n$ and $\tau_m = \mu[2(1 - n)/(1 - 2n)]^{n-1}$.

---

[1] The location of the maximum at $k = 1$ is a matter of convenience only.

The material on which the example in [1] is based, although broadly similar to materials in the subclass described by conditions (i) - (iv) in that its shear stress response curve rises to a peak at $k = 1$ and then declines, does not in fact belong to that subclass. It fails to be smooth enough to satisfy condition (i), and violates the strict inequality on the right in condition (iii) for $0<k<1$.

2. The small-scale nonlinear crack problem

Let $\mathcal{R}$ be the three-dimensional domain consisting of the exterior of a plane infinite strip of width $2c$. Introduce cartesian coordinates x_1, x_2, x_3 in such a way that this strip, which represents a crack, lies in the plane $x_2 = 0$, the x_3-axis being parallel to the edges of the crack and the origin midway between the edges. The cross-section $\mathcal{L}$ of $\mathcal{R}$ in the plane $x_3 = 0$ is evidently the exterior of the segment $-c \le x_1 \le c$ of the x_1-axis.

Suppose that the interior of a body of incompressible material characterized by (1.1) occupies the domain $\mathcal{R}$ in an undeformed configuration, and suppose further that, in the absence of body forces, the solid is subjected at infinity to a simple shear parallel to the edges of the crack.[1] The displacement components u_i must thus satisfy[2]

$$u_\alpha = o(1)\,, \quad u_3 = kx_2 + o(1) \quad \text{as} \quad x_\beta x_\beta \to \infty\,, \tag{2.1}$$

where the nonnegative constant k is the amount of applied shear. The

---

[1] This is the loading case known as "Mode III" in the terminology of fracture mechanics.

[2] Latin and Greek subscripts have the respective ranges (1, 2, 3) and (1, 2), repeated subscripts are summed, and a subscript preceded by a comma indicates differentiation with respect to the corresponding x-coordinate.

deformed faces of the crack are to remain free of traction.

For materials governed by the strain energy density (1.1), it is shown in [2] that the field equations and boundary conditions associated with the crack problem described above are consistent with the assumption that $u_\alpha \equiv 0$ and $u_3 = u(x_1, x_2)$ on $\mathcal{R}$, corresponding to a state of anti-plane shear with out-of-plane displacement $u(x_1, x_2)$. Moreover, the three-dimensional boundary-value problem is reducible, as shown in [2], to the following two-dimensional problem for u on the cross-sectional domain $\mathcal{D}$:

$$[W'(I_1)u_{,\alpha}]_{,\alpha} = 0 \quad \text{on } \mathcal{D} , \tag{2.2}$$

with

$$I_1 = 3 + |\nabla u|^2 , \quad |\nabla u|^2 = u_{,\alpha} u_{,\alpha} , \tag{2.3}$$

and

$$u(x_1, x_2) = kx_2 + o(1) \text{ as } x_\alpha x_\alpha \to \infty , \tag{2.4}$$

$$u_{,2}(x_1, 0\pm) = 0 \quad \text{for } -c < x_1 < c . \tag{2.5}$$

It is also shown in [2] that the components of true stress τ_{ij} satisfy

$$\tau_{3\alpha} = \tau_{\alpha 3} = 2W'(I_1)u_{,\alpha} , \quad \tau_{33} = 2W'(I_1)|\nabla u|^2 , \tag{2.6}$$

$$\tau_{\alpha\beta} = 0 , \tag{2.7}$$

with I_1 given by (2.3).

When the Baker-Ericksen inequality holds, as we assume here,

it is possible to show that the differential equation (2.2) is elliptic at a solution u and at a point (x_1, x_2) if and only if

$$W'(3+k^2)+2k^2W''(3+k^2)>0 \quad , \quad k=|\nabla u(x_1,x_2)| \quad . \tag{2.8}$$

In view of (1.6), this condition for ellipticity is equivalent to the assertion that the response curve in simple shear must have positive slope at an amount of shear equal to the magnitude of the local displacement gradient $\nabla u(x_1, x_2)$. It follows that (2.2) can never suffer a loss of ellipticity if the response function $\tau(k)$ for simple shear is monotone strictly increasing. On the other hand, for the class of materials satisfying conditions (i) - (iv) at the end of the preceding section, (2.2) will lose ellipticity whenever $|\nabla u(x_1, x_2)| \geq 1$. In particular, for the power-law materials characterized by (1.10), (1.11), a loss of ellipticity is possible only if $n<1/2$.

In the presence of a potential loss of ellipticity, it is natural to seek the solution of the boundary-value problem (2.2) - (2.5) in a class of functions whose smoothness is less than that which one would otherwise naturally demand. In fact we shall merely require that u be continuous and have piecewise continuous first and second partial derivatives on $\mathcal{B}$. In addition u is to be bounded inside any circle centered at a crack-tip. Finally, the limits $\nabla u(x_1, 0\pm)$ must exist and be continuous for $-c<x_1<c$.

The preceding smoothness requirements allow for the possibility of finite jump discontinuities in ∇u — and hence also in the stresses τ_{3i} — across curves in $\mathcal{B}$. It is necessary to stipulate that across such a curve $\mathcal{S}$, $W'(I_1)\partial u/\partial n$ shall be continuous[1], where I_1 is given by (2.3) and

[1] This is equivalent to the requirement that the tractions be continuous across $\mathcal{S}$, which in turn is demanded by equilibrium. See Section 1 of [1] and Section 3 of [3].

$\partial u/\partial n$ is a derivative of u normal to $\mathscr{S}$.

For small values of the amount of applied shear k, one would expect that, away from the crack-tips, the solution of the foregoing boundary-value problem would be well-approximated by the solution of the corresponding linearized problem.[1] In fact, arguments sketched in [1] and [2][2] suggest that, for small k, an approximation to the solution of (2.2) - (2.5) which is uniformly valid near the right crack-tip is obtained by replacing the domain $\mathscr{D}$ with the domain $\tilde{\mathscr{D}}$ exterior to the nonpositive x_1-axis (see Fig. 3), requiring (2.2) to hold on $\tilde{\mathscr{D}}$, enforcing the free surface condition (2.5) on the semi-infinite crack $-\infty < x_1 < 0$, $x_2 = 0$, and matching u and its first derivatives at infinity to the corresponding near-field quantities calculated from the exact solution of the original problem according to the linearized theory. This leads to the small-scale nonlinear crack problem in which one seeks a solution u of (2.2) on $\tilde{\mathscr{D}}$ subject to the boundary conditions

$$u_{,2}(x_1, 0\pm) = 0 \quad , \quad x_1 < 0 \tag{2.9}$$

and the matching conditions

$$\left.\begin{aligned} &u \sim k(2cr)^{1/2} \sin\frac{\theta}{2} \quad , \\ &u_{,1} \sim -kc(2cr)^{-1/2}\sin\frac{\theta}{2} \quad , \quad u_{,2} \sim kc(2cr)^{-1/2}\cos\frac{\theta}{2} \quad , \\ &\text{as } r \to \infty \quad , \quad -\pi \le \theta \le \pi \quad . \end{aligned}\right\} \tag{2.10}$$

---

[1] Upon linearization, the boundary-value problem (2.2)-(2.5) passes over to the elementary problem for Laplace's equation corresponding to irrotational flow of an inviscid incompressible fluid past a flat plate at a 90° angle of attack.

[2] See also Rice [5].

Here r, θ are polar coordinates at the crack-tip (Fig. 3), so that

$$x_1 = r\cos\theta \ , \quad x_2 = r\sin\theta \ , \quad r \geq 0 \ , \quad -\pi \leq \theta \leq \pi \ . \tag{2.11}$$

Furthermore, u is to satisfy relaxed regularity conditions strictly analogous to those imposed in connection with the original crack problem.

When referred to the dimensionless variables

$$\bar{x}_\alpha = x_\alpha / ck^2 \ , \quad \bar{r} = r/ck^2 \ , \quad \bar{u} = u/ck^2 \ , \tag{2.12}$$

the boundary-value problem (2.2), (2.9), (2.10) assumes the following non-dimensional form in which k does not appear explicitly:

$$[W'(3 + |\bar{\nabla}\bar{u}|^2)\bar{u}_{,\alpha}]_{,\alpha} = 0 \quad \text{on} \quad \tilde{\mathcal{S}} \ , \tag{2.13}$$[1]

$$\bar{u}_{,2}(\bar{x}_1, 0\pm) = 0 \ , \quad x_1 < 0 \ , \tag{2.14}$$

$$\left.\begin{aligned} &\bar{u} \sim (2\bar{r})^{1/2}\sin\frac{\theta}{2} \ , \\ &u_{,1} \sim -(2r)^{-1/2}\sin\frac{\theta}{2} \ , \quad u_{,2} \sim (2r)^{-1/2}\cos\frac{\theta}{2} \ , \\ &\text{as} \quad r \to \infty \end{aligned}\right\} \tag{2.15}$$

The foregoing small-scale nonlinear crack problem was solved in [2] for the limiting elliptic case $n = 1/2$ of a power-law material governed by (1.10), (1.11), (see Fig. 1), and in [1] for the material described by (1.12), (1.13), (Fig. 2).

---

[1] Subscripts preceded by a comma are now understood to indicate partial derivatives with respect to the dimensionless coordinates $\bar{x}_\alpha$, and $\bar{\nabla}$ stands for the gradient operator with components $\partial/\partial\bar{x}_\alpha$.

3. An algorithm for the construction of solutions to the displacement equation of equilibrium.

A formal algorithm for the construction of a solution to the small-scale nonlinear crack problem (2.13)-(2.15) can be generated with the help of a hodograph transformation, in which the first derivatives of $\bar{u}$ are introduced as new independent variables, and one is led to an explicitly solvable linear boundary-value problem in the hodograph plane for the Legendre transform of $\bar{u}$. For materials which remain elliptic at all deformations, the mapping between the physical and hodograph planes is one-to-one, and the formal procedure indeed produces an exact solution which is infinitely smooth on $\tilde{\mathcal{D}}$. This analysis is carried out in detail in [2] for the limiting elliptic case $n = 1/2$ of the power-law material (1.10).

In [1] the formal hodograph scheme is applied to the boundary-value problem (2.13)-(2.15) for the case of a material defined through (1.12). In this instance, a loss of ellipticity occurs and is accompanied by a breakdown in the invertibility of the hodograph transformation. As shown in [1], even in these circumstances the formal hodograph procedure can be used to find solutions of the differential equation (2.13). These can in turn be combined to construct a solution of relaxed smoothness to the boundary-value problem.

We shall not repeat the description of the hodograph transformation here; instead we merely cite from [1] the resulting formal algorithm and analyze it for incompressible materials governed by (1.1) and satisfying conditions (i) - (iv) stated near the end of Section 1. Let $\tau(k)$ be the shear-stress response function for such a material, and define functions

P and Q by

$$P(\rho) = \int_{\rho}^{\infty} \frac{dt}{t^2 \bar{\tau}(t)} \quad , \quad Q(\rho) = -\rho P'(\rho) \quad , \quad \rho > 0 \quad , \tag{3.1}$$

where

$$\bar{\tau}(t) = \tau(t)/\mu \quad . \tag{3.2}$$

According to the hodograph scheme, the formal solution $\bar{u}$ of the boundary-value problem (2.13)-(2.15) is given implicitly by

$$\bar{u}(\bar{x}_1, \bar{x}_2) = -\rho Q(\rho)\cos\varphi \quad , \quad \bar{r} > 0 \quad , \quad -\pi \le \theta \le \pi \quad , \tag{3.3}$$

where for given $(\bar{x}_1, \bar{x}_2)$ or $(\bar{r}, \theta)$, ρ and φ are to be determined from

$$\left.\begin{aligned} \bar{x}_1 &= \bar{r}\cos\theta = P(\rho) - Q(\rho)\cos^2\varphi \quad , \\ \bar{x}_2 &= \bar{r}\sin\theta = -Q(\rho)\sin\varphi\cos\varphi \quad , \quad \rho > 0 \quad , \quad 0 \le \varphi \le \pi \quad . \end{aligned}\right\} \tag{3.4}$$

It can be shown that for an <u>elliptic</u> material, (3.4) are uniquely invertible: for each $\bar{r} > 0$ and each θ in $[-\pi, \pi]$, there are unique values $\rho = \rho(\bar{r}, \theta)$, $\varphi = \varphi(\bar{r}, \theta)$ with $\rho > 0$ and $0 \le \varphi \le \pi$ such that (3.4) hold. Substitution of these values of ρ, φ into (3.3) furnishes the solution $\bar{u}$.

For the materials of interest here, (3.4) will in general fail to be uniquely invertible for certain values of $(\bar{x}_1, \bar{x}_2)$. The first step in constructing a solution to the small-scale nonlinear crack problem (2.13)-(2.15)

---

[1] Note that (1.16) assures the convergence of the integral in the definition P.

consists in determining the number of roots (ρ, φ) of (3.4) for each value of $(\bar{x}_1, \bar{x}_2)$.

A geometrical version of this issue is arrived at by observing that (3.4) may be written in the equivalent alternative form

$$\left.\begin{aligned} \bar{x}_1 &= \bar{r}\cos\theta = a(\rho) - b(\rho)\cos 2\varphi \\ \bar{x}_2 &= \bar{r}\sin\theta = -b(\rho)\sin 2\varphi \ , \\ & 0 \le \varphi \le \pi \ , \quad \rho > 0 \ , \end{aligned}\right\} \tag{3.5}$$

where

$$a(\rho) = P(\rho) - \tfrac{1}{2}Q(\rho) \ , \quad b(\rho) = \tfrac{1}{2}Q(\rho) \ . \tag{3.6}$$

From (3.1), (3.2), (1.6) and (1.3) it follows that $b(\rho) > 0$ for $\rho > 0$, so that (3.5) represents, for each fixed $\rho > 0$, the parametric equations of a circle $\Gamma(\rho)$ centered at $\bar{x}_1 = a(\rho)$, $\bar{x}_2 = 0$ with radius $b(\rho)$. The cartesian equation for this circle is

$$\Gamma(\rho): \ [\bar{x}_1 - a(\rho)]^2 + \bar{x}_2^2 = b^2(\rho) \ . \tag{3.7}$$

Thus for given values of $\bar{x}_1$ and $\bar{x}_2$, (3.4) has a solution (ρ_*, φ_*) with $\rho_* > 0$, $0 \le \varphi_* \le \pi$, if and only if the circle $\Gamma(\rho_*)$ passes through the point $(\bar{x}_1, \bar{x}_2)$. Moreover if (ρ_*, φ_*) and (ρ_*, φ_{**}) satisfy (3.4) for given $(\bar{x}_1, \bar{x}_2)$, then $\varphi_* = \varphi_{**}$. Thus the <u>number</u> of admissible roots (ρ_*, φ_*) of (3.4) coincides with the number of circles $\Gamma(\rho)$ which pass through the given point $(\bar{x}_1, \bar{x}_2)$ or, equivalently, with the number of roots ρ_* of (3.7).

Let $\tilde{\mathfrak{D}}_*$ be a subdomain of $\tilde{\mathfrak{D}}$ on which ρ_* is a twice continuously differentiable positive function of $(\bar{x}_1, \bar{x}_2)$ satisfying (3.7). Note that for such a ρ_*,

$$a(\rho_*) - b(\rho_*) \leq \bar{x}_1 \leq a(\rho_*) + b(\rho_*) \quad , \tag{3.8}$$

since the left and right members of these inequalities are the abscissas of the intercepts of $\Gamma(\rho_*)$ with the $\bar{x}_1$-axis. Define φ_* through

$$\cos\varphi_* = -\operatorname{sgn}\bar{x}_2 \left[\frac{a(\rho_*) + b(\rho_*) - \bar{x}_1}{2b(\rho_*)}\right]^{1/2} \quad , \quad 0 \leq \varphi_* \leq \pi \quad . \tag{3.9}$$[1]

One shows easily that ρ_*, φ_* satisfy (3.4) on $\tilde{\mathfrak{D}}_*$. Further, if φ_* is twice continuously differentiable on $\tilde{\mathfrak{D}}_*$, the function $\bar{u}$ defined on $\tilde{\mathfrak{D}}_*$ by

$$\bar{u}(x_1, x_2) = -\rho_*(\bar{x}_1, \bar{x}_2) Q(\rho_*(\bar{x}_1, \bar{x}_2)) \cos\varphi_*(\bar{x}_1, \bar{x}_2) \tag{3.10}$$

can be shown by direct calculation to be a solution of the partial differential equation (2.13) on $\tilde{\mathfrak{D}}_*$.

In the next section we investigate the roots ρ_* of (3.7) and their domains of definition $\tilde{\mathfrak{D}}_*$.

4. Geometry of the circles $\Gamma(\rho)$

In order to investigate the roots ρ of (3.7), we need some properties of the functions $a(\rho)$ and $b(\rho)$ which, according to (3.7), determine the circles $\Gamma(\rho)$.

From the definitions (3.6) and (3.1) it follows that

---

[1] $\operatorname{sgn}\bar{x}_2$ is one if $\bar{x}_2 > 0$, zero if $\bar{x}_2 = 0$ and minus one if $\bar{x}_2 < 0$.

$$a(\rho) = \int_{\rho}^{\infty} \frac{dt}{t^2 \bar{\tau}(t)} - \frac{1}{2\rho\bar{\tau}(\rho)} \quad , \quad b(\rho) = \frac{1}{2\rho\bar{\tau}(\rho)} \quad , \quad \rho > 0 \quad , \tag{4.1}$$

$$a'(\rho) = \frac{\rho\bar{\tau}'(\rho) - \bar{\tau}(\rho)}{2\rho^2\bar{\tau}^2(\rho)} \quad , \quad b'(\rho) = -\frac{\rho\bar{\tau}'(\rho) + \bar{\tau}(\rho)}{2\rho^2\bar{\tau}^2(\rho)} \quad , \quad \rho > 0 \quad , \tag{4.2}$$

and hence in particular that

$$a'(\rho) - b'(\rho) = \frac{\bar{\tau}'(\rho)}{\rho\bar{\tau}^2(\rho)} \quad , \quad \rho > 0 \quad . \tag{4.3}$$

Invoking (1.15), one finds from (4.2) that

$$a'(\rho) < 0 \quad , \quad b'(\rho) < 0 \quad , \quad \rho > 0 \quad , \tag{4.4}$$

while (4.3), (1.14) lead to

$$a'(\rho) - b'(\rho) \begin{cases} > 0 \quad , \quad 0 < \rho < 1 \quad , \\ = 0 \quad , \quad \rho = 1 \quad , \\ < 0 \quad , \quad \rho > 1 \quad . \end{cases} \tag{4.5}$$

We shall also require the asumptotic properties of $a(\rho)$, $b(\rho)$ for large and small ρ. The asymptotics for large k of $\tau(k)$ given by (1.16), (1.17) lead via (4.1) to the following estimates for $a(\rho)$, $b(\rho)$:

If $\tau_\infty > 0$: as $\rho \to \infty$,

$$\left.\begin{aligned} a(\rho) &\sim \frac{\mu}{2\tau_\infty}\frac{1}{\rho} - \frac{\mu h \epsilon}{2\tau_\infty^2(2-\epsilon)}\frac{1}{\rho^{2-\epsilon}} \quad , \\ b(\rho) &\sim \frac{\mu}{2\tau_\infty}\frac{1}{\rho} - \frac{\mu h}{2\tau_\infty^2}\frac{1}{\rho^{2-\epsilon}} \quad . \end{aligned}\right\} \tag{4.6}$$

If $\tau_\infty = 0$: as $\rho \to \infty$

$$a(\rho) \sim \frac{\mu(2-\epsilon)}{2h\epsilon} \frac{1}{\rho^\epsilon} \quad , \quad b(\rho) \sim \frac{\mu}{2h} \frac{1}{\rho^\epsilon} \quad . \tag{4.7}$$

From (1.6), (1.2), (3.2) one finds the behavior of $\bar{\tau}(k)$ for small k to be given by

$$\left.\begin{aligned} \bar{\tau}(k) &\sim k - dk^3 \quad \text{as} \quad k \to 0 \quad , \\ d &= -2W''(3)/\mu \quad . \end{aligned}\right\} \tag{4.8}$$

Ruling out a degeneracy, we shall assume

$$d > 0 \quad . \tag{4.9}$$[1]

Using (4.8), (4.9) in (4.1) leads to

$$a(\rho) \sim -d \log \rho \quad , \quad b(\rho) \sim \frac{1}{2\rho^2} \quad \text{as} \quad \rho \to 0+ \quad . \tag{4.10}$$

From (4.6), (4.7) it may be noted that in either of the cases $\tau_\infty > 0$ or $\tau_\infty = 0$, one has

$$a(\rho) \to 0 \quad , \quad b(\rho) \to 0 \quad \text{as} \quad \rho \to \infty \quad , \tag{4.11}$$

while from (4.10) it follows that

$$a(\rho) \to +\infty \quad , \quad b(\rho) \to +\infty \quad \text{as} \quad \rho \to 0+ \quad . \tag{4.12}$$

On the other hand, (4.10) also shows that

---

[1] The fact that $d \geq 0$ is a consequence of (1.15).

$$a(\rho) - b(\rho) \to -\infty \quad \text{as} \quad \rho \to 0+ \quad . \tag{4.13}$$

From (4.4), (4.12) and (4.11) one infers that $a(\rho)$ and $b(\rho)$ decrease monotonically from $+\infty$ at $\rho = 0+$ to zero at $\rho = +\infty$. In particular, both functions are positive for $0 < \rho < \infty$.

According to (4.13), (4.5) and (4.11), $a(\rho) - b(\rho)$ increases monotonically from $-\infty$ at $\rho = 0+$ to a maximum at $\rho = 1$ and then decreases steadily to zero at $\rho = +\infty$ (Fig. 4). Since the maximum value of $a(\rho) - b(\rho)$ is necessarily positive, one has

$$a(1) - b(1) > 0 \quad . \tag{4.14}$$

Finally it is clear that there is a unique number ρ_0 such that $0 < \rho_0 < 1$ and

$$a(\rho_0) - b(\rho_0) = 0 \quad . \tag{4.15}$$

The circles $\Gamma(\rho)$ of (3.7) are centered at $\bar{x}_1 = a(\rho)$, $\bar{x}_2 = 0$, have radius $b(\rho)$ and intersect the $\bar{x}_1$-axis at $\bar{x}_1 = a(\rho) - b(\rho)$ and at $\bar{x}_1 = a(\rho) + b(\rho)$. As ρ increases from zero to one, the center and right $\bar{x}_1$-intercept of $\Gamma(\rho)$ more from $\bar{x}_1 = +\infty$ to the left, while the left $\bar{x}_1$-intercept moves to the right. By (4.15), the left intercept of $\Gamma(\rho_0)$ is at the origin. The circle $\Gamma(1)$, which plays a major role in the analysis to follow, is centered at $\bar{x}_1 = a(1)$, $\bar{x}_1 = 0$, has radius $b(1) = \mu/2\tau_m$, and intersects the $\bar{x}_1$-axis at positive values of $\bar{x}_1$.

As ρ continues to increase from unity, the center and right $\bar{x}_1$-intercept continue to move to the left, and the radius continues to decrease, but the left intercept $\bar{x}_1 = a(\rho) - b(\rho)$ now moves to the left as well (Fig. 5). For very large values of ρ, $\Gamma(\rho)$ is centered very slightly

to the right of the origin and has a small radius.

Two circles $\Gamma(\rho)$ corresponding to values of ρ both of which are less than one do not intersect, but this is not necessarily the case when both values of ρ are greater than one. It is thus not surprising to find that the subfamily of circles $\Gamma(\rho)$ for which $\rho \geq 1$ possesses an envelope. This envelope, which is of decisive importance in the study of the roots ρ of (3.7), is a curve which is tangent at each of its points to one of the circles $\Gamma(\rho)$, $\rho \geq 1$. To find this curve analytically, we first define

$$F(\rho;\bar{x}_1,\bar{x}_2) = [\bar{x}_1 - a(\rho)]^2 + \bar{x}_2^2 - b^2(\rho) \quad , \quad \rho > 0 \ , \ -\infty < \bar{x}_\alpha < \infty \quad . \tag{4.16}$$

The envelope then consists of those points $(\bar{x}_1,\bar{x}_2)$ for which there is a $\rho > 0$ such that

$$F(\rho;\bar{x}_1,\bar{x}_2) = 0 \ \text{ and } \ \frac{\partial F}{\partial \rho}(\rho;\bar{x}_1,\bar{x}_2) = 0 \quad . \tag{4.17}$$

Substitution from (4.16) into (4.17) leads directly to parametric equations for the envelope $\mathcal{L}$:

$$\mathcal{L}: \ \bar{x}_1 = e_1(\rho) \ , \ \bar{x}_2 = \pm [e_2(\rho)]^{1/2} \quad , \quad \rho \geq 1 \ , \tag{4.18}$$

where the functions $e_1(\rho)$, $e_2(\rho)$ are defined <u>for all</u> $\rho > 0$ by[1]

[1] Although only the values of $e_1(\rho)$, $e_2(\rho)$ for $\rho \geq 1$ enter into the parametric equations for $\mathcal{L}$, their values for $0 < \rho < 1$ will be needed later.

$$\left.\begin{aligned} e_1(\rho) &= \frac{a(\rho)a'(\rho) - b(\rho)b'(\rho)}{a'(\rho)} \quad , \\ e_2(\rho) &= \frac{b^2(\rho)}{[a'(\rho)]^2}[a'(\rho) - b'(\rho)][a'(\rho) + b'(\rho)] \quad , \quad 0<\rho<\infty \quad . \end{aligned}\right\} \tag{4.19}$$

Only those circles $\Gamma(\rho)$ for which $\rho \geq 1$ participate in the formation of the envelope because, by (4.4), (4.5), $e_2(\rho) \geq 0$ for $\rho \geq 1$ but $e_2(\rho) < 0$ for $0 < \rho < 1$. Thus $\bar{x}_2$ as given in (4.18) is real only for $\rho \geq 1$.

The envelope $\mathcal{E}$ is symmetric about the $\bar{x}_1$-axis, consisting of an upper and a lower branch as indicated by the sign alternative in (4.18). From (4.4), (4.5), (4.19) and (4.14) one finds that $e_1(\rho) > 0$ for $\rho \geq 1$, so that $\mathcal{E}$ lies in the half-plane[1] $\bar{x}_1 \geq 0$. Moreover, $e_1(1) = a(1) - b(1)$ and $e_2(1) = 0$, so that each branch of $\mathcal{E}$ "begins" when $\rho = 1$ at the left $\bar{x}_1$-intercept of $\Gamma(1)$. A more detailed inspection of $e_1(\rho)$, $e_2(\rho)$ near $\rho = 1$ shows that $\mathcal{E}$ has a vertical tangent at $\rho = 1$ *and its radius of curvature* there is $b(1)$. Thus $\mathcal{E}$ osculates with $\Gamma(1)$ at the left $\bar{x}_1$-intercept of this circle.

As $\rho \to +\infty$, the two points on $\mathcal{E}$ which correspond to ρ tend to the origin, as one sees easily from the asymptotic behavior of $e_1(\rho)$ and $e_2(\rho)$ for large ρ deducible from (4.6) or (4.7), according as $\tau_\infty > 0$ or $\tau_\infty = 0$. In fact, it can be shown that the upper and lower branches of $\mathcal{E}$ approach the origin with vertical tangents as $\rho \to \infty$, provided $\tau_\infty > 0$. If $\tau_\infty = 0$, the upper and lower branches of $\mathcal{E}$ are asymptotically tangent as $\rho \to +\infty$ to the lines $\bar{x}_2 = \pm \frac{1}{2}\epsilon(1-\epsilon)^{-1/2}\bar{x}_1$, where, according to (1.16), ϵ is the material parameter controlling the rate of descent of the shear-stress response curve at large amounts of shear.

---

[1] The origin (which would "correspond" to $\rho = \infty$) is taken to be a point of $\mathcal{E}$.

From (4.19) one finds that

$$e_1'(\rho) = a'(\rho)c(\rho) \quad , \quad e_2'(\rho) = 2b(\rho)b'(\rho)c(\rho) \quad , \quad \rho > 0 \quad , \tag{4.20}$$

where

$$c = 1 - \left(\frac{b'}{a'}\right)^2 + \frac{bb'a''}{(a')^3} - \frac{bb''}{(a')^2} \quad . \tag{4.21}$$

By (4.18), (4.20), the slope $d\bar{x}_2/d\bar{x}_1$ of $\mathcal{L}$ therefore satisfies

$$\bar{x}_2 \frac{d\bar{x}_2}{d\bar{x}_1} = \frac{b(\rho)b'(\rho)}{a'(\rho)} > 0 \text{ for every } \rho \text{ such that } c(\rho) \neq 0 \quad . \tag{4.22}$$

Thus on the upper (lower) branch of $\mathcal{L}$, $\bar{x}_2$ is a monotone strictly increasing (decreasing) function of $\bar{x}_1$ on any arc of $\mathcal{L}$ which includes only points for which $c(\rho) \neq 0$. At values of ρ for which $c(\rho) = 0$, $\mathcal{L}$ has a cusp.

By (4.21), (4.1), (4.5), (4.3), (1.18) and (3.2), one has

$$c(1) = \frac{b(1)}{[b'(1)]^2}[a''(1) - b''(1)] = \frac{2\tau''(1)}{\tau_m} \quad , \tag{4.22}$$

so that by the last of (1.14),

$$c(1) < 0 \quad . \tag{4.23}$$

It then follows that $c(\rho) < 0$ when ρ is near unity, and hence, by (4.18), (4.20), (4.4), $\bar{x}_1$ at first increases along $\mathcal{L}$ as ρ increases from $\rho = 1$. But as $\rho \to \infty$, the corresponding points on $\mathcal{L}$ tend to the origin, and thus $\bar{x}_1$ is ultimately decreasing. One concludes that $c(\rho)$ must change sign at least once for $1 < \rho < \infty$. If the material is such that for <u>all</u> $\rho > 0$, only one such change of sign occurs, then there is a unique number $\rho_c > 1$

such that

$$c(\rho)<0\ ,\ 0<\rho<\rho_c\ ;\ c(\rho_c)=0\ ;\ c(\rho)>0\ ,\ \rho>\rho_c\ . \qquad (4.24)^1$$

When (4.24) holds, one may infer from (4.20) that $e_1(\rho)$ and $e_2(\rho)$ increase monotonically with ρ for $0<\rho<\rho_c$, attain maximum values at $\rho=\rho_c$, and thereafter decrease monotonically with ρ. The asymptotic behavior of $e_1(\rho)$, $e_2(\rho)$, which can be determined from (4.6) or (4.7), (4.10) and (4.19), is such that $e_1(\rho)$ and $e_2(\rho)$ both tend to $-\infty$ as $\rho\to 0+$, and both tend to zero as $\rho\to+\infty$. The zero of $e_1(\rho)$ lies between $\rho=\rho_0$ and $\rho=1$. The graphs of $e_1(\rho)$ and $e_2(\rho)$ are thus as sketched in Fig. 6.

In the analysis to follow, it will be assumed that the material under consideration satisfies the "one-cusp condition" (4.24).[2] At the end of this section, we shall discuss the interpretation of this condition in terms of the shear-stress response curve of the material. In the final section, we shall comment briefly on the effect of relaxing the restriction (4.24).

Suppose (4.24) holds, and let $D(\rho)\geq 0$ be the distance from the center of the circle $\Gamma(1)$ to the points on $\mathscr{L}$ corresponding to ρ. A direct calculation gives

$$D(\rho)D'(\rho)=a'(\rho)[a(\rho)-a(1)]c(\rho)\ ,\ \rho\geq 1\ , \qquad (4.25)$$

so that $D'(\rho)<0$ for $1<\rho<\rho_c$, $D'(\rho_c)=0$, and $D'(\rho)>0$ for $\rho>\rho_c$. Thus as ρ increases from $\rho=1$, the corresponding point on, say, the upper

---

[1] The asymptotic behavior of $c(\rho)$ as $\rho\to 0+$ guarantees that $c(\rho)<0$ for ρ near zero.

[2] Hence, each branch of $\mathscr{L}$ has only one cusp.

branch of $\mathscr{L}$ moves closer to the center of $\Gamma(1)$ until it reaches the cusp, where $D(\rho)$ has a minimum.[1] The point then moves away from the cusp — which lies inside $\Gamma(1)$ — in such a way as to increase its distance from the center of $\Gamma(1)$, eventually crossing $\Gamma(1)$ and approaching the origin.

By a similar argument, one can show that all points of $\mathscr{L}$ except the origin lie in the interior of the circle $\Gamma(\rho_0)$ through the origin.

When (4.24) holds, it can be shown that there are no points of inflection on those portions of the upper or lower branches of $\mathscr{L}$ for which $1 \le \rho < \rho_c$, but the remaining part of each branch has at least one point of inflection. It is also possible to prove that there are no double points on $\mathscr{L}$ when the one-cusp condition holds.

A qualitative sketch of $\mathscr{L}$ is shown in Fig. 7 for $\tau_\infty > 0$ (Case A) as well as for $\tau_\infty = 0$ (Case B).

One can show that the envelope $\mathscr{L}$ is precisely the set of points $(\bar{x}_1, \bar{x}_2)$ at which the Jacobian determinant of the physical coordinates with respect to the hodograph coordinates vanishes. It is therefore analogous to a "limit line" in gas dynamics.[2]

We have not found a satisfactory interpretation of the one-cusp condition (4.24). One <u>can</u> show that $c(\rho)$ vanishes at $\rho = \rho_c > 1$ if and only if the curve representing the <u>square</u> of the shear stress τ in simple shear as a function of the <u>square</u> of the amount of shear ρ has a point of inflection at $\rho = \rho_c$. The presence of more than one cusp on each branch of the envelope $\mathscr{L}$ would therefore correspond to "terracing" in the

---

[1] One can show that $\mathscr{L}$ is tangent to $\Gamma(\rho_c)$ at the cusps.

[2] See §105 of [6].

declining portion of the latter curve ($\rho > 1$).

It can be verified that the power-law materials (1.10), (1.11) for $0 < n < 1/2$ satisfy the one-cusp condition (4.24).

5. Elliptic and hyperbolic solutions of the differential equation

We turn now to the question of the number of roots $\rho > 0$ of (3.7), or equivalently, of the number of positive zeros of F in (4.16) as a function of ρ.

First, suppose that $\bar{x}_1 = \bar{x}_2 = 0$, and observe from (4.16) that

$$F(\rho; 0, 0) = [a(\rho) + b(\rho)][a(\rho) - b(\rho)] \quad , \quad \rho > 0 \quad . \tag{5.1}$$

Since $a(\rho) + b(\rho) > 0$ for $\rho > 0$ and $a(\rho) - b(\rho)$ vanishes only at ρ_0 (see (4.15)), it follows that the only zero of $F(\rho; 0, 0)$ is ρ_0.

Next, assume that $\bar{x}_1^2 + \bar{x}_2^2 > 0$. From (4.11), (4.16), one sees that

$$F(+\infty; \bar{x}_1, \bar{x}_2) = \bar{x}_1^2 + \bar{x}_2^2 > 0 \quad , \tag{5.2}$$

while (4.10), (4.16) yield

$$F(0+; \bar{x}_1, \bar{x}_2) = -\infty \quad . \tag{5.3}$$

Thus for any given $(\bar{x}_1, \bar{x}_2)$, there is at least one positive zero ρ of $F(\rho; \bar{x}_1, \bar{x}_2)$. Note that this result does not depend on the one-cusp condition (4.24).

In order to investigate the number of zeros of F, it is convenient to record first some properties of this function. From (4.16), (4.19) one obtains

$$\frac{\partial F}{\partial \rho}(\rho;\bar{x}_1\bar{x}_2) = -2a'(\rho)[\bar{x}_1 - e_1(\rho)] \quad , \quad \rho>0 \ , \quad -\infty<\bar{x}_\alpha,<\infty \tag{5.4}$$

Thus by (4.4), the graph of F vs. ρ for given $(\bar{x}_1,\bar{x}_2)$ has a horizontal tangent when ρ is such that $\bar{x}_1 = e_1(\rho)$. One sees from Fig. 6, which depends on (4.24), that when $\bar{x}_1 \le 0$, there is precisely one such horizontal tangent — located at a value of ρ between zero and one. If $0<\bar{x}_1<e_1(\rho_c)$, two horizontal tangents occur at, say, $\rho=\hat{\rho}_1$, $\rho=\hat{\rho}_2$ with $\hat{\rho}_1<\rho_c<\hat{\rho}_2$. When $\hat{\rho}_1>1$, both $\hat{\rho}_1$ and $\hat{\rho}_2$ correspond to points on $\mathcal{E}$ which are intersections of $\mathcal{E}$ with the vertical line through the point $(\bar{x}_1,\bar{x}_2)$. When $\hat{\rho}_1<1$, only $\hat{\rho}_2$ refers to a point on $\mathcal{E}$ with this property.[1] If $\bar{x}_1 = e_1(\rho_c)$, there is a horizontal tangent in the graph of F only at $\rho=\rho_c$, and if $\bar{x}_1>\rho_c$, there are no horizontal tangents.

Equations (5.4), (4.16) and (4.19) show that, at a horizontal tangent of F,

$$F(\hat{\rho};\bar{x}_1,\bar{x}_2) = \bar{x}_2^2 - e_2(\hat{\rho}) \quad , \quad \frac{\partial F}{\partial \rho}(\hat{\rho};\bar{x}_1,\bar{x}_2) = 0 \ . \tag{5.5}$$

From the graph of $e_2(\rho)$ in Fig. 6, it is clear that $e_2(\rho)<0$ if $\rho<1$, so that $F(\hat{\rho};\bar{x}_1,\bar{x}_2)>0$ at a horizontal tangent for which $\hat{\rho}<1$. If $\hat{\rho}\ge 1$ in (5.5), then $F(\hat{\rho};\bar{x}_1,\bar{x}_2)$ is positive, zero or negative according as the point $(\bar{x}_1, |\bar{x}_2|)$ lies above, at or below that point on the upper branch of the envelope $\mathcal{E}$ which corresponds to $\hat{\rho}$. The latter point is a point of intersection of $\mathcal{E}$ with the vertical line through $(\bar{x}_1,\bar{x}_2)$.

From (4.16) we observe that $F(1;\bar{x}_1,\bar{x}_2)$ is positive, zero or negative according as $(\bar{x}_1,\bar{x}_2)$ lies outside, on or inside the circle $\Gamma(1)$. Note that

---

[1] Recall that $\mathcal{E}$ contains no points corresponding to values of $\rho<1$ (see (4.18)).

for each fixed ρ and $\bar{x}_1$, $F(\rho;\bar{x}_1,\bar{x}_2)$ is a monotone increasing function of $\bar{x}_2$ for $\bar{x}_2>0$.

The preceding considerations lead to the following conclusions concerning the dependence of the number and location of the zeros of F on the point $(\bar{x}_1,\bar{x}_2)$:

Table 1

Location of $(\bar{x}_1,\bar{x}_2)$	Number of zeros of F in $(0,1)$	Number of zeros of F in $(1,\infty)$
outside $\mathcal{L}$, outside $\Gamma(1)$	1	0
outside $\mathcal{L}$, inside $\Gamma(1)$	0	1
inside $\mathcal{L}$, outside $\Gamma(1)$	1	2
inside $\mathcal{L}$, inside $\Gamma(1)$	0	3

One observes in particular that, at any point $(\bar{x}_1,\bar{x}_2)$ which lies outside $\mathcal{L}$, there is a unique zero of F, while at any point $(\bar{x}_1,\bar{x}_2)$ in the interior of $\mathcal{L}$, there are three distinct zeros.

If, at a given value $(\bar{x}_1^0,\bar{x}_2^0)$ of $(\bar{x}_1,\bar{x}_2)$, $\dot{\rho}$ is a zero of F, the implicit function theorem assures the existence of a function $\rho_*(\bar{x}_1,\bar{x}_2)$, defined and smooth in a neighborhood of $(\bar{x}_1^0,\bar{x}_2^0)$, such that $F(\rho_*(\bar{x}_1,\bar{x}_2);\bar{x}_1,\bar{x}_2)=0$ in this neighborhood, unless $\partial F/\partial\rho$ vanishes at $\dot{\rho}$, $\bar{x}_1^0,\bar{x}_2^0$. Thus differentiability of ρ_* can break down at $(\bar{x}_1,\bar{x}_2)$ only if $(\bar{x}_1,\bar{x}_2)$ coincides with the point on the envelope $\mathcal{L}$ that corresponds to $\dot{\rho}$. Since there are no points on $\mathcal{L}$ corresponding to values of $\rho<1$, no such breakdown in smoothness can occur if $\dot{\rho}<1$.

We now define two functions ρ_1, ρ_2 on the $(\bar{x}_1,\bar{x}_2)$-plane as follows:

$$\rho_1(\bar{x}_1,\bar{x}_2) = \text{the smallest zero of } F(\rho;\bar{x}_1,\bar{x}_2)\ , \tag{5.6}$$

$$\rho_2(\bar{x}_1, \bar{x}_2) = \text{the largest zero of } F(\rho; \bar{x}_1, \bar{x}_2) \ . \tag{5.7}$$

Since F has only one zero for points $(\bar{x}_1, \bar{x}_2)$ which lie strictly outside $\mathcal{L}$, one has $\rho_1 = \rho_2$ in the exterior of $\mathcal{L}$. From (5.1), (4.15) one has $\rho_1(0,0) = \rho_2(0,0) = \rho_0$; ρ_1 is continuous at the origin, but ρ_2 is not. In fact, one has $\rho_2(\bar{x}_1, 0) \to \rho_0$ as $\bar{x}_1 \to 0-$, while $\rho_2(\bar{x}_1, 0) \to +\infty$ as $\bar{x}_1 \to 0+$. Also, $\rho_1 = \rho_2 = \rho_c$ if $(\bar{x}_1, \bar{x}_2)$ coincides with either cusp, and ρ_1 , ρ_2 are continuous at the cusps. One can show that ρ_1 suffers jump discontinuities at all points on that arc of the envelope $\mathcal{L}$ which joins the cusps by way of the left $\bar{x}_1$-intercept of $\Gamma(1)$, except for the cusps themselves. Except for points on this arc of $\mathcal{L}$, ρ_1 is three times continuously differentiable. On the other hand, ρ_2 has jump discontinuities at all points of that branch of $\mathcal{L}$ which joins the cusps via the origin, the cusps excluded, and ρ_2 has continuous third derivatives elsewhere. Both ρ_1 , ρ_2 are even functions of $\bar{x}_2$ for each $\bar{x}_1$.

One infers from the foregoing discussion that

$$\left.\begin{aligned} &\rho_1 = \rho_2 < 1 \text{ outside both } \mathcal{L} \text{ and } \Gamma(1) \ , \\ &\rho_1 = \rho_2 > 1 \text{ outside } \mathcal{L} \text{ but inside } \Gamma(1) \ , \end{aligned}\right\} \tag{5.8}$$

$$\left.\begin{aligned} &\rho_1 > 1 \ , \ \rho_2 > 1 \text{ inside both } \mathcal{L} \text{ and } \Gamma(1) \ , \\ &\rho_0 < \rho_1 < 1 \ , \ \rho_2 > 1 \text{ inside } \mathcal{L} \text{ but outside } \Gamma(1) \ , \end{aligned}\right\} \tag{5.9}$$

and

$$\rho_0 < \rho_1 < \rho_c \ , \ \rho_2 > \rho_c \text{ inside } \mathcal{L} \ . \tag{5.10}$$

As $\bar{x}_2 \to 0$ for fixed $\bar{x}_1$, one shows easily from (5.6), (5.7) and (4.16) that $\rho_1(\bar{x}_1, 0)$ and $\rho_2(\bar{x}_1, 0)$ satisfy

$$\left.\begin{aligned} a(\rho_1(\bar{x}_1,0)) - b(\rho_1(\bar{x}_1,0)) &= \bar{x}_1 \quad \text{for } -\infty < \bar{x}_1 \le a(1) - b(1) , \\ a(\rho_1(\bar{x}_1,0)) + b(\rho_1(\bar{x}_1,0)) &= \bar{x}_1 \quad \text{for } a(1) - b(1) < \bar{x}_1 < \infty , \end{aligned}\right\} \tag{5.11}$$

$$\left.\begin{aligned} a(\rho_2(\bar{x}_1,0)) - b(\rho_2(\bar{x}_1,0)) &= \bar{x}_1 \quad \text{for } -\infty < \bar{x}_1 \le 0 , \\ a(\rho_2(\bar{x}_1,0)) + b(\rho_2(\bar{x}_1,0)) &= \bar{x}_1 \quad \text{for } 0 < \bar{x}_1 < \infty . \end{aligned}\right\} \tag{5.12}$$

Bearing (3.9), (3.10) and the second of (3.6) in mind, we now define functions $\bar{u}_1(\bar{x}_1, \bar{x}_2)$, $\bar{u}_2(\bar{x}_1, \bar{x}_2)$ for all $(\bar{x}_1, \bar{x}_2)$ by

$$\left.\begin{aligned} \bar{u}_\alpha &= \operatorname{sgn} \bar{x}_2 \rho_\alpha \{ 2b(\rho_\alpha)[a(\rho_\alpha) + b(\rho_\alpha) - \bar{x}_1] \}^{1/2} , \\ & \alpha = 1, 2 \ , \ \text{no sum} . \end{aligned}\right\} \tag{5.13}$$[1]

Note that $u_1 = u_2$ on the exterior of the envelope $\mathcal{E}$. From (5.11), (5.12), (5.13) one sees that

$$\bar{u}_1(\bar{x}_1, 0+) - \bar{u}_1(\bar{x}_1, 0-) \begin{cases} \neq 0 & \text{for } -\infty < \bar{x}_1 \le a(1) - b(1) , \\ = 0 & \text{for } a(1) - b(1) < \bar{x}_1 < \infty , \end{cases} \tag{5.14}$$

where

---

[1] Since $b(\rho_\alpha) > 0$, the fact that $\bar{x}_1$ lies between the $\bar{x}_1$-intercepts of $\Gamma(\rho_\alpha)$ assures that the radical in (5.13) is real.

$$\bar{u}_2(\bar{x}_1, 0+) - u_2(\bar{x}_1, 0-) \begin{cases} \neq 0 & \text{for } -\infty < \bar{x}_1 \leq 0 \ , \\ = 0 & \text{for } 0 < \bar{x}_1 < \infty \ . \end{cases} \tag{5.15}$$

Thus $\bar{u}_1$ is continuous at points on the $\bar{x}_1$-axis to the right of the left $\bar{x}_1$-intercept of $\Gamma(1)$ but discontinuous across the crack $\bar{x}_1 \leq 0$, $\bar{x}_2 = 0$, as well as across the segment $0 \leq \bar{x}_1 \leq a(1) - b(1)$ of the $\bar{x}_1$-axis ahead of the crack. In contrast, $\bar{u}_2$ is discontinuous across the crack but remains continuous at all points of the $\bar{x}_1$-axis ahead of the crack-tip. These observations, together with the remarks following (5.7) concerning the loci of points of discontinuity of ρ_1 and ρ_2 , permit the determination of the maximal domains of smoothness for $\bar{u}_1$ and $\bar{u}_2$. Let $\tilde{\mathcal{D}}_1$ consist of the set of all points in the domain $\tilde{\mathcal{D}}$ which lie neither on the line segment $0 < \bar{x}_1 \leq a(1) - b(1)$, $\bar{x}_2 = 0$ nor on that arc of the envelope $\mathcal{E}$ which joins the two cusps by way of the point $\bar{x}_1 = a(1) - b(1)$, $\bar{x}_2 = 0$. Similarly, let $\tilde{\mathcal{D}}_2$ be the set of those points in $\tilde{\mathcal{D}}$ which do not lie on that arc of $\mathcal{E}$ which joins the two cusps via the origin.[1] Then $\bar{u}_\alpha$ is three times continuously differentiable on $\tilde{\mathcal{D}}_\alpha$. Moreover, one can show by direct calculation based on (5.13), (4.16) (and the fact that ρ_1 , ρ_2 are zeros of F) that $\bar{u}_\alpha$ satisfies the differential equation (2.13) on $\tilde{\mathcal{D}}_\alpha$. In the process of carrying out this calculation, one finds that

$$\bar{u}_{\alpha,1} = -\operatorname{sgn} \bar{x}_2 \rho_\alpha \left[\frac{a(\rho_\alpha) + b(\rho_\alpha) - \bar{x}_1}{2b(\rho_\alpha)} \right]^{1/2} \quad \text{on } \tilde{\mathcal{D}}_\alpha \ , \tag{5.16}$$

[1] It is understood that the cusps themselves do not belong either to $\tilde{\mathcal{D}}_1$ or to $\tilde{\mathcal{D}}_2$.

$$\bar{u}_{\alpha,2} = \rho_\alpha \left[\frac{\bar{x}_1 - a(\rho_\alpha) + b(\rho_\alpha)}{2b(\rho_\alpha)} \right]^{1/2} \quad \text{on } \tilde{\mathcal{D}}_\alpha \ , \tag{5.17}$$

and hence that

$$|\nabla \bar{u}_\alpha| = \rho_\alpha \quad \text{on } \tilde{\mathcal{D}}_\alpha \ . \tag{5.18}$$

In view of (5.8), (5.9) and (5.18), one concludes that the differential equation (2.13) is <u>elliptic</u> at the solution $\bar{u}_1$ at those points of $\tilde{\mathcal{D}}_1$ which lie outside $\Gamma(1)$ and <u>hyperbolic</u> in that part of $\tilde{\mathcal{D}}_1$ which lies inside $\Gamma(1)$. Similarly, (2.13) is elliptic at the solution $\bar{u}_2$ at those points of $\tilde{\mathcal{D}}_2$ which lie outside both $\mathcal{L}$ and $\Gamma(1)$ ($\bar{u}_2$ and $\bar{u}_1$ in fact coincide there), but hyperbolic at any point of $\tilde{\mathcal{D}}_2$ which lies either in the interior of $\Gamma(1)$ or in the interior of $\mathcal{L}$.

One has $\rho_1(\bar{x}_1, \bar{x}_2) = \rho_2(\bar{x}_1, \bar{x}_2)$ outside $\mathcal{L}$ and as $\bar{r} = \sqrt{\bar{x}_1^2 + \bar{x}_2^2} \to 0$, their common value tends to zero. In fact, from (4.10), (4.16), (5.6) and (5.7) it follows that

$$\rho_1(\bar{x}_1, \bar{x}_2) = \rho_2(\bar{x}_1, \bar{x}_2) \sim 2^{-1/2} \bar{r}^{-1/2} \quad \text{as } \bar{r} \to \infty \ , \tag{5.19}$$

and hence from (4.10), (5.13) and (5.19) that

$$\bar{u}_1(\bar{x}_1, \bar{x}_2) = \bar{u}_2(\bar{x}_1, \bar{x}_2) \sim (2\bar{r})^{1/2} \sin\frac{\theta}{2} \quad \text{as } \bar{r} \to \infty \ . \tag{5.20}$$

Thus $\bar{u}_1$ and $\bar{u}_2$ satisfy the condition at infinity (2.15) posed as a part of the small-scale nonlinear crack problem.

From (5.17) with $\alpha = 1$, one obtains

$$\bar{u}_{1,2}(\bar{x}_1, 0\pm) = \rho_1(\bar{x}_1, 0)\left[\frac{\bar{x}_1 - a(\rho_1(\bar{x}_1, 0)) + b(\rho_1(\bar{x}_1, 0))}{2b(\rho_1(\bar{x}_1, 0))}\right]^{1/2} . \qquad (5.21)$$

But according to the first of (5.11), the numerator in the bracket in (5.21) vanishes for $\bar{x}_1 < a(1) - b(1)$, so that

$$\bar{u}_{1,2}(\bar{x}_1, 0\pm) = 0 \quad , \quad -\infty < \bar{x}_1 < a(1) - b(1) \quad . \qquad (5.22)$$

Thus, in particular, $\bar{u}_1$ satisfies the free surface condition (2.14) along the crack[1] $-\infty < \bar{x}_1 < 0$, $\bar{x}_2 = 0$.

Neither $\bar{u}_1$ nor $\bar{u}_2$ alone can serve as a solution of the small-scale nonlinear crack problem, since neither is smooth enough throughout $\mathfrak{D}$. In the next section we shall show how they can be pieced together to construct the desired solution.

It may be remarked that a third solution $\bar{u}_3$ of (2.13) differing from $\bar{u}_1$ and $\bar{u}_2$ only at points inside $\mathscr{L}$, could be constructed with the help of that zero of F which, for $(\bar{x}_1, \bar{x}_2)$ inside $\mathscr{L}$, lies between ρ_1 and ρ_2. We shall not need this solution in what follows, and so we do not investigate its features here.

6. Solution of the small-scale nonlinear crack problem.

Here we construct a continuous, piecewise smooth solution $\bar{u}$ of the boundary-value problem (2.13)-(2.15); $\bar{u}$ will coincide with $\bar{u}_1$ on a subset of $\mathfrak{D}$ and with $\bar{u}_2$ on the remainder of $\mathfrak{D}$. We first observe that, because of the discontinuities in $\bar{u}_1$ and $\bar{u}_2$, $\bar{u}$ will be required to coincide with $\bar{u}_1$ at those points of $\mathfrak{D}$ which lie near that branch of $\mathscr{L}$ which joins the cusps

[1] The solution $\bar{u}_2$ also has vanishing normal derivative at $\bar{x}_2 = 0\pm$ for $-\infty < \bar{x}_1 < 0$.

by way of the origin, while $\bar{u}$ and $\bar{u}_2$ will coincide near the remaining branch of $\mathcal{L}$, as well as in the vicinity of the segment $0<\bar{x}_1<a(1)-b(1)$ of the $\bar{x}_1$-axis. This suggests that we attempt to "match" $\bar{u}_1$ and $\bar{u}_2$ across two as yet undetermined curves $\mathcal{S}^+$ and $\mathcal{S}^-$ (Fig. 8) that are symmetrically situated with respect to the $\bar{x}_1$-axis, start at the origin, terminate at the cusps, and otherwise lie wholly within the interior of $\mathcal{L}$. This matching must assure the continuity of $\bar{u}$ and of the traction across the two curves to be found. We shall show that there are unique "shocks" $\mathcal{S}^+$ and $\mathcal{S}^-$ with the desired properties. As either of these curves is traversed, $\bar{u}$ and its tangential derivative remain continuous, while the normal derivative of $\bar{u}$ jumps – despite the prevailing continuity of traction across $\mathcal{S}^+$ and $\mathcal{S}^-$.

Momentarily taking for granted the existence of $\mathcal{S}^+$ and $\mathcal{S}^-$, let $\mathcal{T}^{(1)}$ stand for the set of those points in $\mathcal{T}$ which lies strictly outside the closed curve formed by $\mathcal{S}^+$, $\mathcal{S}^-$ and that branch of $\mathcal{L}$ which connects the cusps by way of the point $\bar{x}_1 = a(1) - b(1)$, $\bar{x}_2 = 0$ (Fig. 8), while $\mathcal{T}^{(2)}$ consists of the interior of this closed curve ($\mathcal{T}^{(2)}$ is shaded in Fig. 8). Define $\bar{u}$ on $\mathcal{T}$ by first setting

$$\bar{u} = \begin{cases} \bar{u}_1 & \text{on } \mathcal{T}^{(1)}, \\ \bar{u}_2 & \text{on } \mathcal{T}^{(2)}, \end{cases} \tag{6.1}$$

and then extending the definition of $\bar{u}$ to all points of $\mathcal{S}^+$, $\mathcal{S}^-$ (except the origin) and the right branch of $\mathcal{L}$ by continuity. It is clear from (5.20) that $\bar{u}$ satisfies the condition (2.15) at infinity and from (5.22) that it

also satisfies the boundary condition (2.14) on the crack faces. Finally, $\bar{u}$ is smooth and satisfies the differential equation (2.13) on $\tilde{\mathcal{L}}$ except at points of $\mathscr{S}^+$ and $\mathscr{S}^-$. We shall ultimately show that $\bar{u}$ remains bounded as $\bar{r} \to 0$.

It therefore remains only to establish the existence of curves $\mathscr{S}^+$ and $\mathscr{S}^-$ with the required properties. We consider $\mathscr{S}^+$ only; the existence of $\mathscr{S}^-$ then follows from symmetry.

Suppose for the moment that there is such a curve $\mathscr{S}^+$, and let $(\bar{x}_1, \bar{x}_2)$ be a point on it. Since $\mathscr{S}^+$ lies on or inside $\mathscr{L}$, one has from (5.10) that

$$0 < \rho_1(\bar{x}_1, \bar{x}_2) \le \rho_c , \quad \rho_2(\bar{x}_1, \bar{x}_2) \ge \rho_c , \quad (\bar{x}_1, \bar{x}_2) \in \mathscr{S}^+ \tag{6.2}$$

Since $\bar{u}$ as given by (6.1), (5.13) is to be continuous at $(\bar{x}_1, \bar{x}_2)$ on $\mathscr{S}^+$, it follows that

$$\rho_2[2b_2(a_2 + b_2 - \bar{x}_1)]^{1/2} = \rho_1[2b_1(a_1 + b_1 - \bar{x}_1)]^{1/2} \quad \text{on } \mathscr{S}^+ , \tag{6.3}$$

where we have set

$$b_\alpha = b(\rho_\alpha) , \quad a_\alpha = a(\rho_\alpha) , \quad \alpha = 1, 2 . \tag{6.4}$$

Since ρ_1, ρ_2 are zeros of $F(\rho; \bar{x}_1, \bar{x}_2)$, one has from (4.16) that

$$(\bar{x}_1 - a_1)^2 + \bar{x}_2^2 = b_1^2 , \quad (\bar{x}_1 - a_2)^2 + \bar{x}_2^2 = b_2^2 \quad \text{on } \mathscr{S}^+ \tag{6.5}$$

If we define g by

$$g(\rho) = \rho^2 b(\rho)[a(\rho) + b(\rho)] , \quad \rho > 0 , \tag{6.6}$$

the result of squaring both sides of (6.3) and solving for $\bar{x}_1$ may be expressed as[1]

$$\bar{x}_1 = \frac{g_2 - g_1}{b_2\rho_2^2 - b_1\rho_1^2} \quad \text{on } \mathscr{S}^+ , \tag{6.7}$$

where

$$g_\alpha = g(\rho_\alpha) , \quad \alpha = 1, 2 . \tag{6.8}$$

Using (6.7) in the first of (6.5) yields

$$\bar{x}_2^2 = b_1^2 - \left[\frac{g_2 - g_1}{b_2\rho_2^2 - b_1\rho_1^2} - a_1 \right]^2 \quad \text{on } \mathscr{S}^+ . \tag{6.9}$$

Substitution from (6.7), (6.9) into the second of (6.5) then leads after some algebra to the conclusion that the values of ρ_1 and ρ_2 on the shock must be related by

$$\Phi(\rho_1, \rho_2) = 0 \quad \text{on } \mathscr{S}^+ , \tag{6.10}$$

where Φ is defined for all $\rho_1 > 0$, $\rho_2 > 0$ by

$$\Phi(\rho_1, \rho_2) = b_1\rho_1^2(a_1 + b_1 - a_2 + b_2) - b_2\rho_2^2(a_2 + b_2 - a_1 + b_1) , \tag{6.11}$$

(recall (6.4)).

The issue of establishing the existence of the solution (6.1) of the

---

[1] Since we are interested only in $\rho_1 > 0$, $\rho_2 > 0$, (6.7) is <u>equivalent</u> to (6.3) and leads to no extraneous results.

small-scale nonlinear crack problem is a matter of the reversibility of the argument leading to (6.10), (6.11). We shall establish below the following six claims:

(i) for every $\rho_1 \in (\rho_0, \rho_c]$, there is a unique root $\rho_2 = \overline{\rho}_2(\rho_1) \geq \rho_c$ of (6.10);

(ii) setting $\rho_2 = \overline{\rho}_2(\rho_1)$ in (6.7), (6.9) supplies a parametric representation of a curve $\mathscr{S}^+$ with tracing parameter ρ_1;

(iii) as $\rho_1 \to \rho_0+$, the corresponding point on $\mathscr{S}^+$ approaches the origin, while as $\rho_1 \to \rho_c-$, the associated point on $\mathscr{S}^+$ moves to the upper cusp;

(iv) except for its endpoints, $\mathscr{S}^+$ lies in the interior of $\mathscr{L}$;

(v) (6.3) holds on $\mathscr{S}^+$ (except at the origin), so that $\overline{u}$ as defined by (6.1) is continuous except at the origin;

(vi) the traction is continuous across $\mathscr{S}^+$ (except at the origin).

In order to analyze the shock equation (6.10), we require a further property of $b(\rho)$ as well as some results pertaining to the function $g(\rho)$ defined in (6.6). From (4.1), (4.2) and (4.4) one finds that

$$[\rho^2 b(\rho)]' = -\rho^2 a'(\rho) > 0 , \quad \rho > 0 , \tag{6.12}$$

so that $\rho^2 b(\rho)$ is an increasing function of ρ. Since by (4.10), $\rho^2 b(\rho) \to 1/2$ as $\rho \to 0+$, it follows that

$$\rho^2 b(\rho) > \frac{1}{2} , \quad \rho > 0 . \tag{6.13}$$

The asymptotic behavior of $g(\rho)$ can be determined from (4.10), (4.6) or (4.7), and (6.6) as

$$g(\rho) \sim \frac{1}{4\rho^2} \quad \text{as} \quad \rho \to 0+ , \tag{6.14}$$

and

$$g(\rho) \sim \frac{\mu^2}{2\tau_\infty^2} \quad \text{as} \quad \rho \to +\infty \quad \text{if} \quad \tau_\infty > 0 \ , \tag{6.15}$$

while

$$g(\rho) \sim \frac{\mu^2}{2h^2\epsilon} \rho^{2(1-\epsilon)} \quad \text{as} \quad \rho \to +\infty \quad \text{if} \quad \tau_\infty = 0 \ . \tag{6.16}$$

The material constants τ_∞ , h and ϵ first appeared in (1.16); note that $0 < \epsilon < 1$.

From (6.6), (6.12) and the first of (4.19) it further follows that

$$g'(\rho) = -\rho^2 a'(\rho) e_1(\rho) \ , \quad \rho > 0 \ . \tag{6.17}$$

According to (6.6), (6.14), (6.17), (4.4) and the graph of $e_1(\rho)$ in Fig.6, $g(\rho)$ must decrease from $+\infty$ at $\rho = 0+$ to a positive minimum at that value of ρ at which $e_1(\rho)$ vanishes, thereafter increasing steadily with ρ . According to (6.15), (6.16) g rises to a finite limit as $\rho \to +\infty$ if $\tau_\infty > 0$, but tends to $+\infty$ as $\rho \to +\infty$ if $\tau_\infty = 0$.

If $\tau_\infty > 0$, there is a unique number $\rho_\infty > 0$ such that

$$g(\rho_\infty) = g(+\infty) = \frac{\mu^2}{2\tau_\infty^2} \ . \tag{6.18}$$

With the help of a cclculation too long to be included here, it is possible to show that

$$\rho_\infty < \rho_0 \ , \tag{6.19}$$

ρ_0 being the zero of $a(\rho) - b(\rho)$ (see (4.15)). Thus

$$g(\rho) < g(\infty) = \frac{\mu^2}{2\tau_\infty^2} \quad \text{for } \rho \geq \rho_0 \text{ if } \tau_\infty > 0 \ . \tag{6.20}$$

A sketch of the graph of $g(\rho)$ is shown in Fig. 9.

We now turn to the function $\Phi(\rho_1, \rho_2)$ introduced in (6.11), from which it is immediately noted that

$$\Phi(\rho_1, \rho_1) = 0 \ , \quad \Phi(\rho_2, \rho_1) = -\Phi(\rho_1, \rho_2) \ . \tag{6.21}$$

We are interested in the behavior of $\Phi(\rho_1, \rho_2)$ as a function of ρ_2, $0 < \rho_2 < \infty$, when ρ_1 is held fixed at a value not less than ρ_0. A straightforward calculation based on (6.11), (6.12) and the first of (4.19) furnishes the identity

$$b_2 \frac{\partial \Phi}{\partial \rho_2}(\rho_1, \rho_2) = a_2'[\Psi(\rho_1, \rho_2) - \Phi(\rho_1, \rho_2)] \ , \quad \rho_1 > 0 \ , \ \rho_2 > 0 \ , \tag{6.22}$$

with Ψ given by

$$\Psi(\rho_1, \rho_2) = (b_2\rho_2^2 - b_1\rho_1^2)e_1(\rho_2) + g_1 - g_2 \ , \quad \rho_1 > 0 \ , \ \rho_2 > 0 \ , \tag{6.23}$$

where $g_\alpha = g(\rho_\alpha)$, g is defined by (6.6), $e_1(\rho)$ is given in (4.19), and we have set $a_2' = a'(\rho_2)$. From (6.23), (6.22), and (6.21) it follows in particular that

$$\Psi(\rho_1, \rho_1) = 0 \ , \quad \rho_1 > 0 \ , \tag{6.24}$$

and

$$\frac{\partial \Phi}{\partial \rho_2}(\rho_1, \rho_1) = 0 \quad , \quad \rho_1 > 0 \quad . \tag{6.25}$$

Differentiating (6.23), (6.22) with respect to ρ_2, setting $\rho_2 = \rho_1$, and making use of (6.12), (6.17), (4.20) yields

$$\frac{\partial^2 \Phi}{\partial \rho_2^2}(\rho_1, \rho_1) = 0 \quad , \quad \rho_1 > 0 \quad . \tag{6.26}$$

Finally, a further differentiation gives

$$\frac{\partial^3 \Phi}{\partial \rho_2^3}(\rho_1, \rho_1) = \frac{-\rho_1^2 (a_1')^3}{b_1} c_1 \quad , \tag{6.27}$$

where $a_1' = a'(\rho_1)$, $c_1 = c(\rho_1)$, and the function c is defined in (4.21). In view of the one-cusp condition (4.24), (6.27) and (4.4) furnish

$$\frac{\partial^3 \Phi}{\partial \rho_2^3}(\rho_1, \rho_1) \begin{cases} < 0 \quad , \quad 0 < \rho_1 < \rho_c \\ = 0 \quad , \quad \rho_1 = \rho_c \\ > 0 \quad , \quad \rho > \rho_c \quad . \end{cases} \tag{6.28}$$

Making use of (6.21), (6.25), (6.26), (6.28) and the appropriate Taylor approximation for $\Phi(\rho_1, \rho_2)$, one can thus determine the local behavior of $\Phi(\rho_1, \rho_2)$ as a function of ρ_2 near the zero $\rho_2 = \rho_1$:

$$\left.\begin{array}{l} \Phi(\rho_1, \rho_2) \text{ decreases with } \rho_2 \text{ at } \rho_2 = \rho_1 \quad \text{if } 0 < \rho_1 < \rho_c \quad , \\ \\ \Phi(\rho_1, \rho_2) \text{ increases with } \rho_2 \text{ at } \rho_2 = \rho_1 \quad \text{if } \rho_1 > \rho_c \quad . \end{array}\right\} \tag{6.29}$$

From (6.23), one finds that

$$\frac{\partial \Psi(\rho_1,\rho_2)}{\partial \rho_2} = (b_2\rho_2^2 - b_1\rho_1^2)a_2'c_2 \ , \ \rho_1>0 \ , \ \rho_2>0 \ , \tag{6.30}$$

where $c_2 = c(\rho_2)$ and $c(\rho)$ is given by (4.21). Invoking the one-cusp condition (4.24), one sees that the graph of $\Psi(\rho_1,\rho_2)$ vs ρ_2 has horizontal tangents only at $\rho_2=\rho_1$ and $\rho_2=\rho_c$. Differentiation of (6.30) with respect to ρ_2 gives, at $\rho_2=\rho_1$,

$$\frac{\partial^2 \Psi}{\partial \rho_2^2}(\rho_1,\rho_1) = -\rho_1^2(a_1')^2c_1 \ , \ \rho_1>0 \ , \tag{6.31}$$

so that, by (4.24),

$$\frac{\partial^2 \Psi}{\partial \rho_2^2}(\rho_1,\rho_1) \begin{cases} >0 \ , & 0<\rho_1<\rho_c \\ =0 \ , & \rho_1=\rho_c \\ <0 \ , & \rho_1>\rho_c \ . \end{cases} \tag{6.32}$$

Next we consider the asymptotic behavior of $\Phi(\rho_1,\rho_2)$ and $\Psi(\rho_1,\rho_2)$ as $\rho_2 \to +\infty$ and as $\rho_2 \to 0+$ for fixed $\rho_1 \geq \rho_0$. It follows easily from (4.6) or (4.7) and (6.11), (6.23), (4.19), (6.6), (6.18) that as $\rho_2 \to \infty$, one has

for $\tau_\infty > 0$:

$$\Phi(\rho_1,\rho_2) \sim \frac{\mu}{2\tau_\infty}(a_1 - b_1)\rho_2 > 0 \quad \text{if } \rho_1>\rho_0 \ , \tag{6.33}$$

$$\Phi(\rho_0,\rho_2) \sim g(\rho_0) - g(\rho_\infty) < 0 \tag{6.34}$$

$$\Psi(\rho_1,\rho_2) \sim g(\rho_1) - g(\rho_\infty) < 0 \quad \text{if } \rho_1 \geq \rho_0 \ , \tag{6.35}$$

for $\tau_\infty = 0$:

$$\Phi(\rho_1, \rho_2) \sim \frac{\mu}{2h}(a_1 - b_1)\rho_2^{2-\epsilon} > 0 \quad \text{if } \rho_1 > \rho_0 \ , \tag{6.36}$$

$$\Phi(\rho_0, \rho_2) \sim -\frac{\mu^2}{2h^2\epsilon}\rho_2^{2(1-\epsilon)} < 0 \tag{6.37}$$

$$\Psi(\rho_1, \rho_2) \sim -\frac{\mu^2}{2h^2(2-\epsilon)}\rho_2^{2(1-\epsilon)} < 0 \quad \text{if } \rho_1 > 0 \ . \tag{6.38}$$

On the other hand, the small-ρ_2 behavior of Φ and Ψ can be deduced with the help of (4.10): as $\rho_2 \to 0+$,

$$\Phi(\rho_1, \rho_2) \sim \frac{1}{2\rho_2^2}(b_1\rho_1^2 - \tfrac{1}{2}) > 0 \ , \quad \rho_1 > 0 \ , \tag{6.39}$$

$$\Psi(\rho_1, \rho_2) \sim \frac{1}{2d\rho_2^4}(b_1\rho_1^2 - \tfrac{1}{2}) > 0 \ , \quad \rho_1 > 0 \ . \tag{6.40}$$

We shall now make use of all of the foregoing properties of Φ and Ψ in order to describe the graphs of $\Psi(\rho_1, \rho_2)$ and $\Phi(\rho_1, \rho_2)$ as functions of ρ_2 , $0 < \rho_2 < \infty$, with ρ_1 fixed, $\rho_0 \le \rho_1 \le \rho_c$. Suppose first $\rho_0 < \rho_1 < \rho_c$. From (6.40) one sees that $\Psi(\rho_1, \rho_2)$ decreases from $+\infty$ at $\rho_2 = 0+$ until it reaches its zero at $\rho_2 = \rho_1$ (see (6.24)), at which point it has a horizontal tangent, according to (6.30). As ρ_2 increases from ρ_1 , $\Psi(\rho_1, \rho_2)$ increases, reaching a maximum at $\rho = \rho_c$, thereafter declining steadily. If $\tau_\infty > 0$, $\Psi(\rho_1, \rho_2)$ approaches a finite negative limit as $\rho_2 \to +\infty$, by (6.35). If $\tau_\infty = 0$, (6.38) shows that $\Psi(\rho_1, \rho_2) \to -\infty$ as $\rho_2 \to +\infty$. The graph of $\Psi(\rho_1, \rho_2)$ vs. ρ_2 for $\rho_0 < \rho_1 < \rho_c$ is shown as the dashed curve

in Fig. 10.

According to (6.22), the graph of $\Phi(\rho_1,\rho_2)$ vs. ρ_2 can have a horizontal tangent only where it crosses the graph of $\Psi(\rho_1,\rho_2)$ vs. ρ_2. By (6.39), (6.22), $\Phi(\rho_1,\rho_2)$ decreases from $+\infty$ at $\rho_2=0+$, remaining less than $\Psi(\rho_1,\rho_2)$ until it vanishes, together with $\Psi(\rho_1,\rho_2)$, at $\rho_2=\rho_1$, where there is a horizontal tangent (see (6.25)). By the first of (6.29), $\Phi(\rho_1,\rho_2)$ is negative and, by (6.22), continues to decrease as ρ_2 increases from ρ_1 until its graph crosses that of $\Psi(\rho_1,\rho_2)$ with a horizontal tangent. As ρ_2 continues to increase, $\Phi(\rho_1,\rho_2)$ then increases monotonically to $+\infty$ (see (6.33) or (6.36)), crossing the ρ_2-axis once and only once at $\rho_2=\rho_2(\bar{\rho}_1)$. The graph of $\Phi(\rho_1,\rho_2)$ vs. ρ_2 for $\rho_0<\rho_1<\rho_c$ is shown as the solid curve in Fig. 10.

For $\rho_1=\rho_0$ or $\rho_1=\rho_c$, it is easily shown that $\Phi(\rho_1,\rho_2)$ vanishes *if and only if* $\rho_2=\rho_1$, *whether* $\tau_\infty>0$ *or* $\tau_\infty=0$.

Thus for $\rho_0<\rho_1\leq\rho_c$, there is a unique root $\rho_2=\bar{\rho}_2(\rho_1)\geq\rho_c$ of (6.10), whether $\tau_\infty>0$ or $\tau_\infty=0$, and claim (i) is established. A detailed study of the behavior of $\bar{\rho}_2(\rho_1)$ shows that $\bar{\rho}_2(\rho_1)$ decreases monotonically as ρ_1 increases, and that

$$\left.\begin{aligned}\bar{\rho}_2(\rho_1)&\to+\infty \quad \text{as } \rho_1\to\rho_0^+ ,\\ \bar{\rho}_2(\rho_1)&\to\rho_c^+ \quad \text{as } \rho_1\to\rho_c^- .\end{aligned}\right\} \tag{6.41}$$

In fact, the asymptotic behavior of $\bar{\rho}_2(\rho_1)$ as $\rho_1\to\rho_0^+$ can be shown to be given by

$$\bar{\rho}_2(\rho_1) \sim \rho_0 \left[\frac{\tau^2(\rho_0) - \tau_\infty^2}{\tau_\infty \tau'(\rho_0)} \right] (\rho_1 - \rho_0)^{-1} \quad \text{if } \tau_\infty > 0 \ . \tag{6.42}$$

Here $\rho_0 < 1$ is the unique zero of $a(\rho) - b(\rho)$ (see (4.15)), $\tau(k)$ is the shear stress[1] in simple shear at an amount of shear k, and τ_∞ is the ultimate stress in simple shear.

If $\tau_\infty = 0$, (6.42) must be replaced by

$$\bar{\rho}_2(\rho_1) \sim \left[\frac{\rho_0 \tau^2(\rho_0)}{\epsilon h \tau'(\rho_0)} \right]^{\frac{1}{\epsilon}} (\rho_1 - \rho_0)^{-\frac{1}{\epsilon}} \ , \ \rho_1 \to \rho_0^+ \ , \ \tau_\infty = 0 \ ; \tag{6.43}$$

here h, ϵ are the material constants introduced in (1.16), (1.17).

If one sets $\rho_2 = \bar{\rho}_2(\rho_1)$ in (6.7), then $\bar{x}_1$ is given as a function of ρ_1 for $\rho_0 < \rho_1 \leq \rho_c$. In order to show that the same substitution in (6.9) furnishes x_2 as a function of ρ_1, it is first necessary to establish that the right side of (6.9) – with $\rho_2 = \bar{\rho}_2(\rho_1)$ – is positive. Let

$$Z(\rho_1, \rho_2) = b_1^2 - \left(\frac{g_2 - g_1}{b_2 \rho_2^2 - b_1 \rho_1^2} - a_1 \right)^2 \ , \ \rho_1 > 0 \ , \ \rho_2 > 0 \ . \tag{6.44}$$

If ρ_1, ρ_2 satisfy (6.10) with Φ given by (6.11), it is possible to show that

$$Z(\rho_1, \rho_2) = \frac{b_1 b_2 \rho_1^2 \rho_2^2}{(b_2 \rho_2^2 - b_1 \rho_1^2)^2} (a_1 - a_2 + b_1 - b_2)(a_1 - a_2 - b_1 + b_2) \ . \tag{6.45}$$

When $\rho_2 > \rho_1$, one has by (4.4) that $a_1 - a_2 + b_1 - b_2 > 0$, so that the sign of

---

[1] Note that $\tau(k)$ is the dimensional shear stress (as distinguished from $\bar{\tau}(k)$ which is nondimensional).

$Z(\rho_1,\rho_2)$ is the same as that of $a_1 - a_2 - b_1 + b_2$, provided (6.10) holds. To determine the latter sign, we first use (6.11), (6.6), and (4.19) in (6.23) to show that, if ρ_1,ρ_2 satisfy (6.10), then

$$\Psi(\rho_1,\rho_2) = \frac{b_2}{a_2'}(a_2' - b_2')(b_2\rho_2^2 - b_1\rho_1^2) - b_2\rho_2^2(a_1 - a_2 - b_1 + b_2) \quad . \qquad (6.46)$$

But according to Fig. 10, $\Psi(\rho_1,\overline{\rho}_2(\rho_1))<0$. Moreover $a_2'<0$ by (4.4), $a_a' - b_2'<0$ if $\rho_2=\overline{\rho}_2(\rho_1)\geq\rho_c>1$ by (4.5), and $b_2\rho_2^2 - b_1\rho_1^2>0$ if $\rho_2>\rho_1$ by (6.12). When these facts are used in (6.46), one concludes that $a_1 - a_2 - b_1 + b_2>0$ when $\rho_2=\overline{\rho}_2(\rho_1)$, and hence that $Z(\rho_1,\overline{\rho}_2(\rho_1))>0$, $\rho_0<\rho_1\leq\rho_c$. It then follows that the right side of (6.9) is positive when $\rho_2=\overline{\rho}_2(\rho_1)$, and hence (6.7), (6.9) with $\rho_2=\overline{\rho}_2(\rho_1)$, $\rho_0<\rho_1\leq\rho_c$ supply parametric equations of a curve $\mathscr{S}^+$ for $\overline{x}_2>0$ (or $\mathscr{S}^-$ if $\overline{x}_2<0$), thus establishing claim (ii).

Equation (6.41) shows that $\overline{\rho}_2(\rho_1)\to+\infty$ as $\rho_1\to\rho_0+$, and thus by (4.6) or (4.7), (6.15) or (6.16), and (6.7), it follows that $\overline{x}_1\to 0+$ on $\mathscr{S}^+$ as $\rho_1\to\rho_0+$. A similar argument, making use of (4.15) as well, shows that $\overline{x}_2\to 0+$ on $\mathscr{S}^+$ as $\rho_1\to\rho_0+$.

On the other hand, as $\rho_1\to\rho_c-$, (6.41) asserts that $\overline{\rho}_2(\rho_1)\to\rho_c+$; (6.17), (6.12), (4.19), (6.7) and L'Hospital's rule then show that $\overline{x}_1\to e_1(\rho_c)$ on $\mathscr{S}^+$. It then follows from (6.9) and (4.19) that $\overline{x}_2\to\sqrt{e_2(\rho_c)}$ on $\mathscr{S}^+$ as $\rho_1\to\rho_c-$. Thus $(\overline{x}_1,\overline{x}_2)$ in $\mathscr{S}^+$ approaches the upper cusp of $\mathscr{L}$ as $\rho_1\to\rho_c-$, and claim (iii) is confirmed.

Suppose that $(\overline{x}_1,\overline{x}_2)$ is an interior point of $\mathscr{S}^+$ corresponding to ρ_1, $\rho_0<\rho_1<\rho_c$. Then (6.10), (6.11), (6.7), (6.9) and (4.16) imply that ρ_1 and $\overline{\rho}_2(\rho_1)$ are both zeros of $F(\rho;\overline{x}_1,\overline{x}_2)$, so that $(\overline{x}_1,\overline{x}_2)$ is a point at which F has more then one zero. By Table 1 of the preceding section,

$(\bar{x}_1, \bar{x}_2)$ cannot lie outside $\mathcal{L}$. If $(\bar{x}_1, \bar{x}_2)$ were <u>on</u> $\mathcal{L}$, then ρ_1 and $\bar{\rho}_2(\rho_1)$ would both be double zeros of F (see (4.17)), which is easily shown not to be the case. Thus $(\bar{x}_1, \bar{x}_2)$ lies inside $\mathcal{L}$, as asserted in claim (iv).

It can be shown directly that (6.10), (6.11), and (6.7) – with $\rho_2 = \bar{\rho}_2(\rho_1)$, $\rho_0 < \rho_1 \leq \rho_c$ – imply (6.3), and hence by (6.1), (5.13), $\bar{u}$ is continuous at all points of $\mathcal{S}^+$ except the origin. This establishes claim (v).

To verify that the traction is continuous across the shock, it is necessary first to determine the slope of $\mathcal{S}^+$. If one sets $\rho_2 = \bar{\rho}_2(\rho_1)$ in (6.10) and then differentiates with respect to ρ_1, one can determine $\bar{\rho}_2'(\rho_1)$ in terms of ρ_1, $\rho_2 = \bar{\rho}_2(\rho_1)$ with the help of the appropriate properties of $a(\rho)$, $b(\rho)$ and $\Phi(\rho_1, \rho_2)$. To find the slope of $\mathcal{S}^+$, it is then only necessary to differentiate (6.7) and (6.9) (with $\rho_2 = \bar{\rho}_2(\rho_1)$) with respect to ρ_1 and substitute for $\bar{\rho}_2'(\rho_1)$ the value determined as outlined above. The resulting formula for the slope can be simplified by using (6.10), (6.11) to eliminate ρ_1, ρ_2 where they appear explicitly. The final form for the slope is then found to be

$$m = \frac{d\bar{x}_2}{d\bar{x}_1} = \frac{b_1 - b_2}{b_1 + b_2} \left[\frac{(a_1 - a_2 + b_1 + b_2)(a_2 - a_1 + b_1 + b_2)}{(a_1 - a_2 - b_1 + b_2)(a_1 - a_2 + b_1 - b_2)} \right]^{1/2}$$

$$\text{on } \mathcal{S}^+, \quad \rho_2 = \bar{\rho}_2(\rho_1), \quad \rho_0 < \rho_1 < \rho_c \,. \tag{6.47}$$

We note in passing that the monotonicity properties of $a(\rho)$, $b(\rho)$ and $\rho^2 b(\rho)$ established in (4.4), (6.12) permit one to conclude that the slope

of $\mathscr{S}^+$ is positive at each of its interior points.[1]

The vector $\underset{\sim}{N}$ with components

$$N_1 = -m(1+m^2)^{-1/2} \quad , \quad N_2 = (1+m^2)^{-1/2} \quad , \tag{6.48}$$

in which m given by (6.47), is a unit normal vector of $\mathscr{S}^+$. By (2.6), (2.7), the only nonvanishing component of traction on a curve in $\mathcal{T}$ with normal $\underset{\sim}{N}$ is the $\bar{x}_3$-component, which is given by

$$t = \tau_{3\beta} N_\beta = 2W'(3 + |\bar{\nabla}\bar{u}|^2)\bar{u}_{,\beta} N_\beta \quad . \tag{6.49}$$

By (1.6), (3.2) and (4.1), this may be written as

$$t = \frac{\mu}{2\rho^2 b(\rho)} \bar{u}_{,\beta} N_\beta \quad , \quad \rho = |\bar{\nabla}\bar{u}| \quad . \tag{6.50}$$

The components $\bar{u}_{,1}$, $\bar{u}_{,2}$ of $\bar{\nabla}\bar{u}$ are discontinuous across $\mathscr{S}^+$, being given by (5.16), (5.17) and (6.1) on the side of $\mathscr{S}^+$ associated with ρ_α , $\alpha = 1,2$. The limiting values of $\bar{u}_{,1}$, $\bar{u}_{,2}$ on the ρ_α-side of $\mathscr{S}^+$ can be expressed entirely in terms of ρ_1 , ρ_2 by substituting for $\bar{x}_1$ in (5.16), (5.17) from (6.7). Since N_1, N_2 are expressed solely in terms of ρ_1, ρ_2 by (6.48), (6.47), the limiting tractions t_1 , t_2 on the two sides of $\mathscr{S}^+$ can then be found in terms of ρ_1, ρ_2 alone by (6.50). In the resulting formulas for t_1 and t_2 , ρ_1, ρ_2 appear explicitly as well as in the arguments of a and b. It is possible to use the shock condition (6.10), (6.11) to eliminate the explicit appearance of ρ_1, ρ_2 . When this is done, one

---

[1] Note that one also requires the fact that $a_1 - a_2 - b_1 + b_2 > 0$ as established in the discussion following (6.46).

finds that $t_1 = t_2$ on $\mathscr{S}^+$, confirming the continuity of traction across $\mathscr{S}^+$ and thus establishing claim (vi).

Geometrically, the shocks $\mathscr{S}^+$ and $\mathscr{S}^-$ are the loci of points of intersection of the circles $\Gamma(\rho_1)$ and $\Gamma(\rho_2)$ as ρ_1 varies from ρ_0 to ρ_c, ρ_2 from $+\infty$ to ρ_c in accordance with the relation $\rho_2 = \bar{\rho}_2(\rho_1)$. These circles are shown schematically in Fig. 8.

7. The field near the crack-tip. Discussion

The local behavior near the crack-tip of the shock $\mathscr{S}^+$ and of the displacement and stresses can be determined from the global solution to the small-scale nonlinear crack problem constructed in the preceding section. We consider first the case of a material for which the ultimate shear stress in simple shear is positive: $\tau_\infty > 0$. To determine the shape of $\mathscr{S}^+$ near the origin, it is easiest to proceed from the expression (6.47) for the slope m. Since $\rho_1 \to \rho_0^+$ and $\rho_2 \to +\infty$ on $\mathscr{S}^+$ as the origin is approached, one can determine the limiting value of $d\bar{x}_2/d\bar{x}_1$ as $\bar{x}_1 \to 0+$ from (6.47) by using the asymptotic results (6.42) and (4.6), along with (4.15), (4.1), (4.3) and (3.2). This leads to

$$\lim_{\bar{x}_1 \to 0+} \frac{d\bar{x}_2}{d\bar{x}_1} = \frac{\tau_\infty}{\sqrt{\tau_0^2 - \tau_\infty^2}} , \qquad \tau_\infty > 0 , \tag{7.1}$$

where $\tau_0 = \tau(\rho_0)$, and, by (4.15), (4.1) and (3.2), ρ_0 is the unique number in $(0, 1)$ such that

$$\int_{\rho_0}^{\infty} \frac{d\rho}{\rho^2 \tau(\rho)} = \frac{1}{\rho_0 \tau(\rho_0)} \quad . \tag{7.2}$$[1]

From (7.1) it follows that $\mathscr{S}^+$ is asymptotically straight at the origin:

$$\bar{x}_2 \sim \frac{\tau_\infty}{\sqrt{\tau_0^2 - \tau_\infty^2}} \bar{x}_1 \quad \text{on } \mathscr{S}^+ \text{ as } \bar{x}_1 \to 0 \, , \; \tau_\infty > 0 \quad . \tag{7.3}$$

Thus $\mathscr{S}^+$ and $\mathscr{S}^-$ subtend a limiting angle $2\theta_0$ at the origin, where $\tan \theta_0 = \tau_\infty (\tau_0^2 - \tau_\infty^2)^{-1/2}$.

To find the limiting value of $u(\bar{x}_1, \bar{x}_2)$ as $(\bar{x}_1, \bar{x}_2)$ approaches the origin from within the domain $\mathfrak{D}^{(1)}$ (i.e. from the elliptic side), one uses (6.1) and (5.13) with $\alpha = 1$ and lets $\rho_1 \to \rho_0^+$. Making use of (4.15), (4.1), (3.2) and (7.3), one obtains

$$\lim_{\bar{r} \to 0} \bar{u}(\bar{x}_1, \bar{x}_2) = \pm \frac{\mu}{\tau_0} \quad \text{as } \bar{r} \to 0 \, , \; \theta_0 < |\theta| \leq \pi \, , \; \tau_\infty > 0 \, , \tag{7.4}$$

where the ambiguous sign is chosen to be the sign of θ. Note that (7.4) confirms that $\bar{u}$ is discontinuous at the origin.

In order to find the limiting value of $\bar{u}$ at the origin from the hyperbolic domain $\mathfrak{D}^{(2)}$, it is necessary first to observe that the second of (6.5), together with (4.6), implies that

$$\rho_2(\bar{x}_1, \bar{x}_2) \sim \frac{\mu}{\tau_\infty} \frac{\cos\theta}{\bar{r}} \quad \text{as } \bar{r} \to 0 \, , \; \tau_\infty > 0 \quad . \tag{7.5}$$

---

[1] One can use (4.15), (6.6), the second of (4.1), and (6.20) with $\rho = \rho_0$ to show that $\tau_0 > \tau_\infty$.

Appealing to (6.1), (5.13) with $\alpha = 2$, letting $\bar{r} \to 0$ and invoking (7.5), one is led to

$$\lim_{\bar{r}\to 0} u(x_1, x_2) = \frac{\mu}{\tau_\infty} \sin\theta \ , \quad -\theta_0 \le \theta \le \theta_0 \ , \ \tau_\infty > 0 \ . \tag{7.6}$$

A graph of the limiting value of $\bar{u}$ vs. θ, for $\tau_\infty > 0$, is shown in Fig. 11. Note that (7.4), (7.6) together show that $\bar{u}$ is bounded near the crack-tip, as originally required.

The corresponding limiting values of the stresses τ_{3i} can be found from (1.6), (1.16), (2.6), (5.16)-(5.18) in an analogous way. The cylindrical components of shearing stress $\tau_{rz} = \tau_{31}\cos\theta + \tau_{32}\sin\theta$ and $\tau_{\theta z} = -\tau_{31}\sin\theta + \tau_{32}\cos\theta$ turn out to satisfy

$$\lim_{\bar{r}\to 0} \tau_{rz} = \begin{cases} 0 \ , & -\theta_0 < \theta < \theta_0 \\ \\ \pm\tau_0 \cos\theta \ , & \theta_0 < |\theta| \le \pi \ , \end{cases} \qquad \tau_\infty > 0 \tag{7.7}$$[1]

$$\lim_{\bar{r}\to 0} \tau_{\theta z} = \begin{cases} \tau_\infty \ , & 0 \le |\theta| < \theta_0 \\ \\ \tau_0 |\sin\theta| \ , & \theta_0 < |\theta| \le \pi \ , \end{cases} \qquad \tau_\infty > 0 \ . \tag{7.8}$$

The ambiguous sign in (7.7) is opposite to the sign of θ. Graphs of these limiting stresses ($\tau_\infty > 0$) are given in Fig. 12, in which θ_0 was chosen to be greater than $\pi/4$.

---

[1] A more refined calculation shows that $\tau_{rz} = O(\bar{r})$ for $-\theta_0 < \theta < \theta_0$.

The axial stress τ_{33} is given asymptotically by

$$\tau_{33} \sim \begin{cases} \dfrac{\mu \cos\theta}{\bar{r}} , & -\theta_0 < \theta < \theta_0 \\ \\ \tau_0 \rho_0 , & \theta_0 < |\theta| \leq \pi , \end{cases} \qquad \text{as } \bar{r} \to 0 , \ \tau_\infty > 0 . \tag{7.9}$$

The limiting behavior as $\bar{r} \to 0$ of $\bar{u}$, τ_{rz}, $\tau_{\theta z}$ and τ_{33} is qualitatively similar to the small-$\bar{r}$ behavior of these quantities as determined in [1] for the small-scale nonlinear crack problem in the case of an incompressible material governed by the shear stress response (1.13). For the displacement and the shearing stresses, this similarity can be seen by comparing Figs. 11, 12 of the present paper with Figs. 7, 8, 9 of [1].

Apart from the presence of the discontinuity in stresses associated with the shock, the above limiting values of displacement and stress also bear a qualitative resemblance to corresponding results obtained in [2] for the "softest" of the elliptic power-law materials (the case $n = 1/2$ in (1.11)).

It is possible to confirm directly the continuity of displacement and traction across $\mathscr{S}^+$ near the origin by making use of (7.3), (7.4) and (7.6)-(7.8).

For the case of a material with $\tau_\infty = 0$, similar – but more involved – arguments which we shall not give here lead to the appropriate crack-tip approximations. In this instance, the shocks $\mathscr{S}^+$ and $\mathscr{S}^-$ are tangent to the $\bar{x}_1$-axis at the origin according to the formula

$$\bar{x}_2 \sim \frac{\mu}{\tau_0} \left(\frac{h}{\mu} \right)^{1/\epsilon} \epsilon^{1/\epsilon} \bar{x}_1^{\,1/\epsilon} \qquad \text{as } \bar{x} \to 0+ \quad \text{on } \mathscr{S}^+ ; \ \tau_\infty = 0 . \tag{7.10}$$

Here $\tau_0 = \tau(\rho_0)$, with ρ_0 determined by (7.2), and h, ϵ are the material constants governing the shear stress response at large shear (see (1.16)); recall that $h>0$, $0<\epsilon<1$.

The limiting value of the displacement $\bar{u}(\bar{x}_1, \bar{x}_2)$ at the origin from within $\tilde{\mathcal{D}}^{(1)}$ (i.e. from the elliptic side) is again given by (7.4), except that now $\theta_0 = 0$, since $\mathcal{L}^+$ and $\mathcal{L}^-$ are tangent to the $\bar{x}_1$-axis at the origin. On the other hand, if the origin is approached along a curve which lies in the hyperbolic domain $\tilde{\mathcal{D}}^{(2)}$, (7.6) must be replaced by

$$\bar{u} \sim \epsilon^{-1/2}\left(\frac{\mu}{h}\right)^{1/\epsilon} 2^{1-1/\epsilon}\left(\frac{2-\epsilon}{\epsilon}\cos\theta + R(\theta)\right)^{1/\epsilon - 1/2} \frac{\sin\theta}{[\cos\theta + R(\theta)]^{1/2}}\bar{r}^{-(1-\epsilon)/\epsilon}$$

$$\text{as } (\bar{x}_1, \bar{x}_2) \to (0,0) \quad \text{inside } \tilde{\mathcal{D}}^{(2)}, \ \tau_\infty = 0, \tag{7.11}$$

where

$$R(\theta) = \left[\frac{(2-\epsilon)^2}{\epsilon^2}\cos^2\theta - \frac{4(1-\epsilon)}{\epsilon^2}\right]^{1/2}. \tag{7.12}$$

With reference to (7.12), one must note that $R(\theta)$ is real for $|\cos\theta| \geq 2(1-\epsilon)^{1/2}/(2-\epsilon)$, and only small values of $|\theta|$ are relevant in (7.11), again because $\mathcal{L}^+$ and $\mathcal{L}^-$ are tangent to the $\bar{x}_1$-axis at the origin.

It can be shown from (7.10), (7.11) that $\bar{u}$ remains bounded as the origin is approached from the hyperbolic domain along any curve that remains between $\mathcal{L}^+$ and $\mathcal{L}^-$. Since according to (7.4) such boundedness clearly prevails for any approach to the origin from the elliptic side, one concludes once again that $\bar{u}$ is bounded near the crack-tip.

The choice $\tau_\infty = 0$, $h = \mu$, $\epsilon = 1/2$ in (1.16) furnishes precisely the

large-k behavior of the material described by (1.13) and treated in [1]. Although this material is not included in the class of materials studied in the present paper, principally because of the lack of smoothness at $k = 1$ in its shear-stress response curve (Fig. 2), it is nevertheless true that setting $\epsilon = 1/2$, $h = \mu$ in (7.10), (7.11), (7.12) reduces (7.10), (7.11) precisely to the corresponding results in [1].[1] This reflects the fact that crack-tip behavior within the hyperbolic region is determined entirely by the large-k behavior of the shear-stress response curve. It is also true that, if one uses $\tau(\rho)$ as given by (1.13) in (7.2) to determine ρ_0, sets $\tau_0 = \tau(\rho_0) = \mu\rho_0$, and uses this in (7.4), the result coincides with the limiting value of $\bar{u}$ from the elliptic side at the origin as determined in [1].

Crack-tip approximations for the stresses in the case $\tau_\infty = 0$ remain the same as for the case $\tau_\infty > 0$ insofar as limiting values from the elliptic side are concerned. Approximations appropriate to an approach to the crack-tip from the hyperbolic domain for $\tau_\infty = 0$ have been found but will not be given here. They, too, reduce to corresponding results in [1] when $\epsilon = 1/2$, $h = \mu$.

As a point on the shock approaches the cusp, the shock "weakens" in the sense that discontinuities in the displacement gradients tend to zero. At the cusp itself, one can determine the field quantities in terms of ρ_c – the value of ρ at which $c(\rho)$ in (4.21) vanishes. A typical formula is that for the displacement at the cusp:

---

[1] See (4.1), (4.2) and (4.9) of [1].

$$\bar{u}_{cusp} = \mu \left\{ -\rho_c^2 \tau(\rho_c) \left[\frac{d}{d\rho} \left(\frac{\tau}{\rho} \right) \right]_{\rho=\rho_c} \right\}^{-1/2} . \qquad (7.13)^1$$

The largest resultant shearing stress $(\tau_{3\alpha}\tau_{3\alpha})^{1/2}$ occurs at points of the circle $\Gamma(1)$ and has the value τ_m (see (1.18)). The axial stress τ_{33} becomes infinite as the crack-tip is approached from within the hyperbolic domain.

The small-scale nonlinear crack problem appears to be substantially more complicated if the one-cusp condition (4.24) fails to hold. If there is more than one cusp on each of the branches of the envelope $\mathcal{L}$, it can be seen that there must be at least three on each branch. The situation sketched schematically in Fig. 13 would seem to be a possible one as regards an envelope $\mathcal{L}$ with three cusps per branch. Among the possibilities suggested by Fig. 13 is one in which the shocks $\mathcal{S}^+$ and $\mathcal{S}^-$ are forked, as indicated by the dashed lines.

In [3], [4] it was proposed that elastostatic shocks should be subject to a certain "dissipation condition" analogous to the requirement of increasing particle entropy across a gas-dynamic shock. For the shocks constructed in [1] in connection with the small-scale nonlinear crack problem for the special material (1.13), it was verified that this dissipation condition was fulfilled when the amount of shear prescribed at infinity is a quasi-statically increasing function of time, corresponding to <u>loading</u> (as distinguished from <u>unloading</u>). We have not investigated the corresponding issue in the more general setting of the present paper.

---

[1] Recall that (1.15) implies $d/d\rho(\tau(\rho)/\rho) < 0$.

References

[1] J.K. Knowles and Eli Sternberg, Discontinuous deformation gradients near the tip of a crack in finite anti-plane shear: an example, Technical Report No. 40, Contract N00014-75-C-0196, Office of Naval Research, to appear in Journal of Elasticity.

[2] J.K. Knowles, The finite anti-plane shear field near the tip of a crack for a class of incompressible elastic solids, International Journal of Fracture, 13, (1977), 611.

[3] J.K. Knowles and Eli Sternberg, On the failure of ellipticity and the emergence of discontinuous deformation gradients in plane finite elastostatics, Journal of Elasticity, 8 (1978), 329.

[4] J.K. Knowles, On the dissipation associated with equilibrium shocks in finite elasticity, Journal of Elasticity, 9 (1979), 131.

[5] J.R. Rice, Stresses due to a sharp notch in a work-hardening elastic-plastic material loaded by longitudinal shear, Journal of Applied Mechanics, 34 (1967), 287.

[6] R. Courant and K.O. Friedrichs, Supersonic flow and shock waves, Interscience, New York, 1948.

$$\tau(k) = \mu\left[1 + \frac{b}{n}k^2\right]^{n-1} k \qquad (0 \le k < \infty)$$

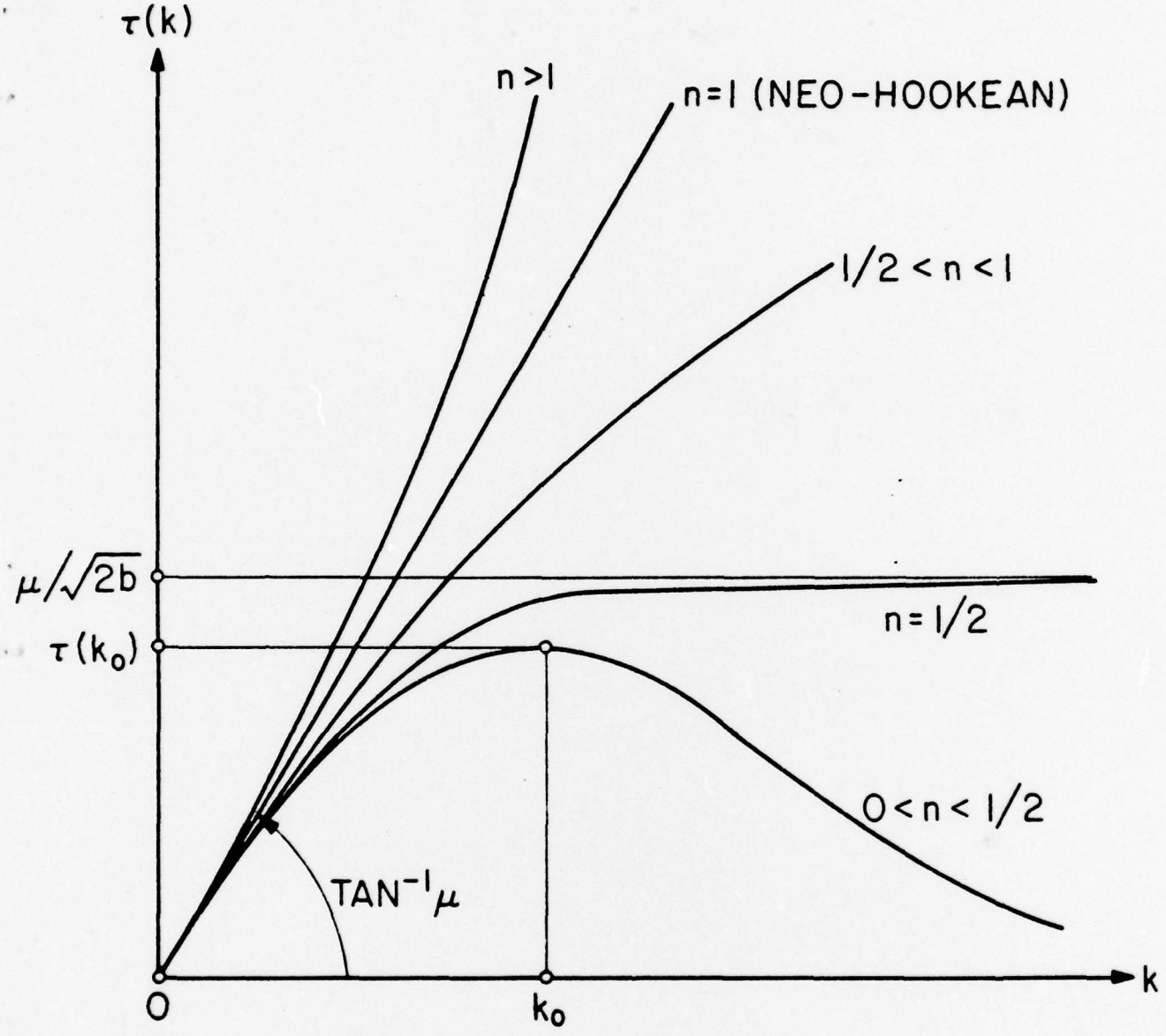

$$k_0 = \sqrt{n/(1-2n)b}, \quad \tau(k_0) = \mu\left[2(1-n)/(1-2n)\right]^{n-1} k_0$$

FIGURE 1. RESPONSE CURVES IN SIMPLE SHEAR FOR POWER-LAW MATERIALS.

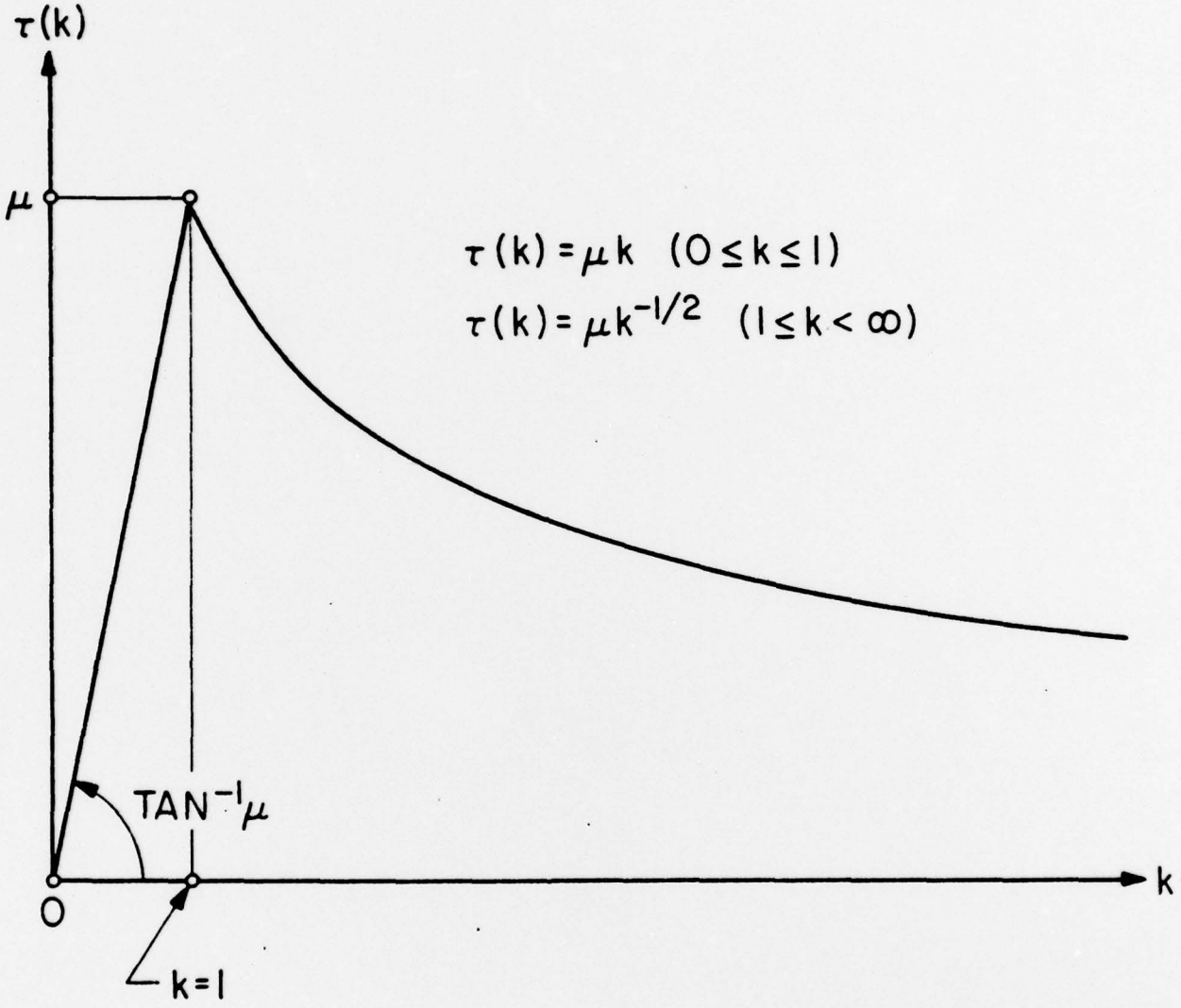

FIGURE 2. RESPONSE CURVE IN SIMPLE SHEAR FOR THE SPECIAL MATERIAL GOVERNED BY EQ. (1.12).

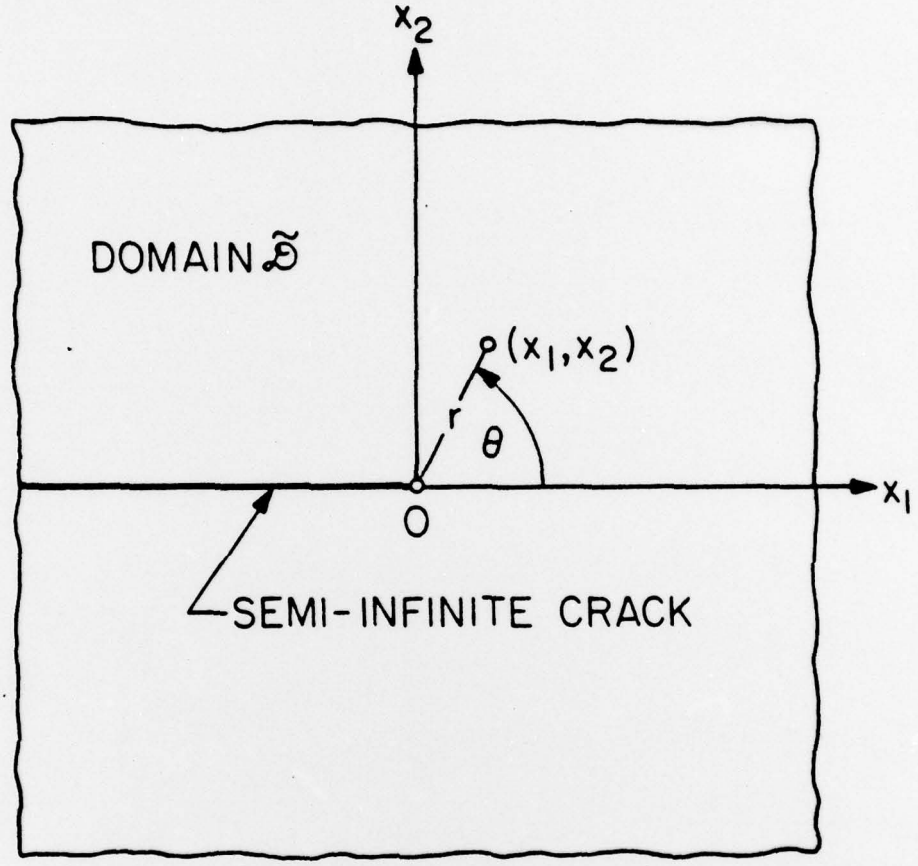

FIGURE 3. SEMI-INFINITE CRACK AND DOMAIN $\tilde{\mathcal{D}}$ FOR SMALL-SCALE NONLINEAR CRACK-PROBLEM.

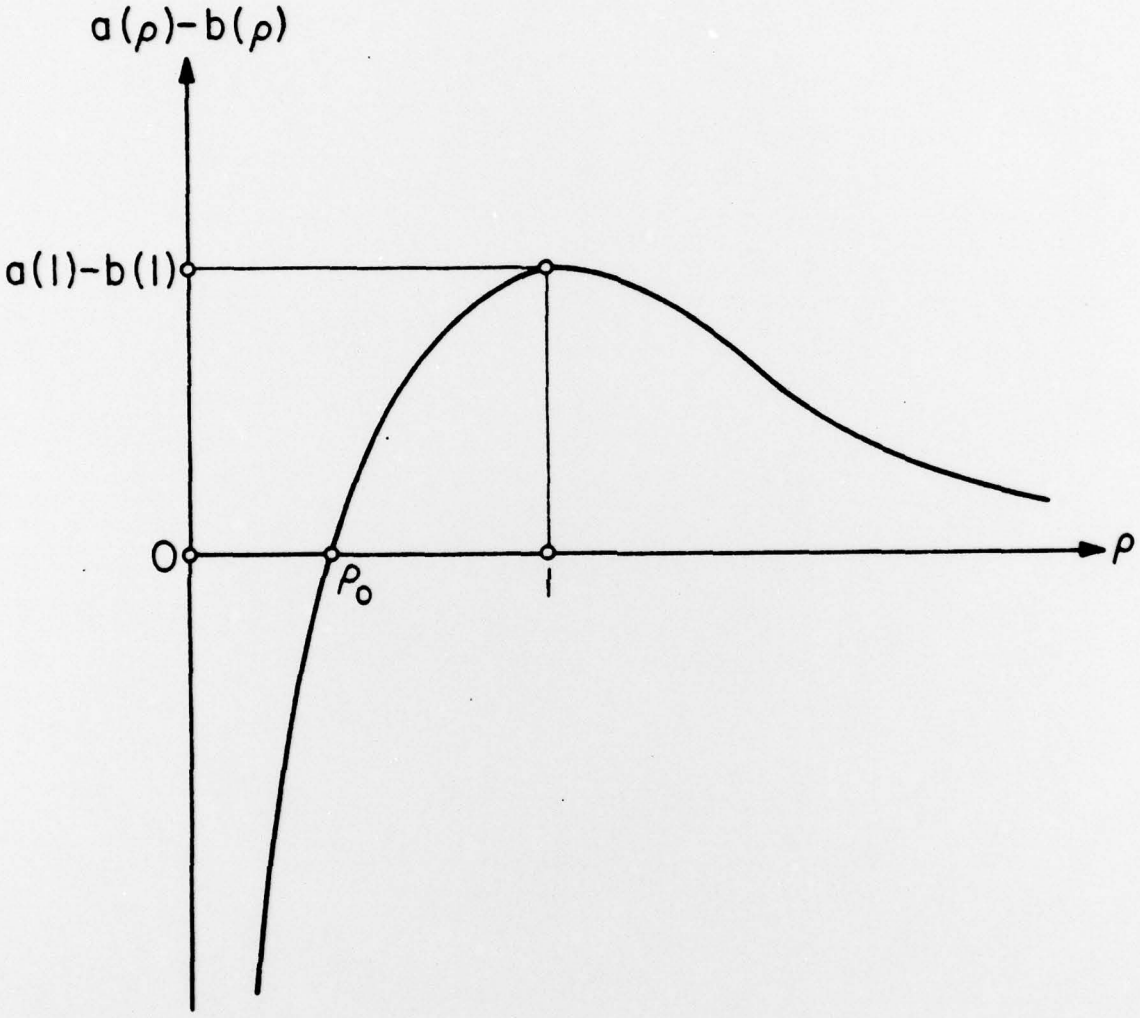

FIGURE 4. QUALITATIVE GRAPH OF $a(\rho)-b(\rho)$.

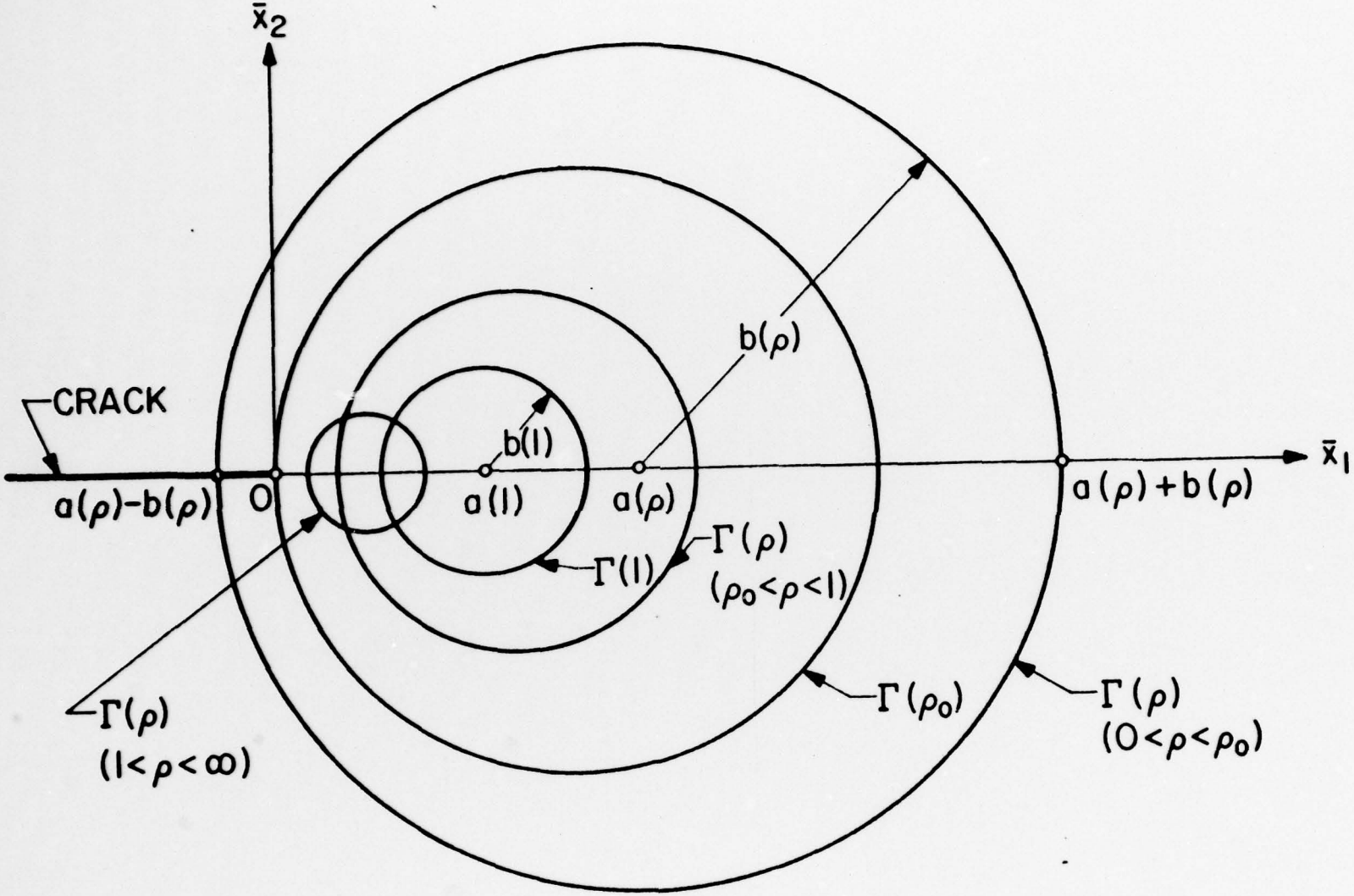

FIGURE 5. SCHEMATIC DIAGRAM OF CIRCLES $\Gamma(\rho)$ $(0<\rho<\infty)$.

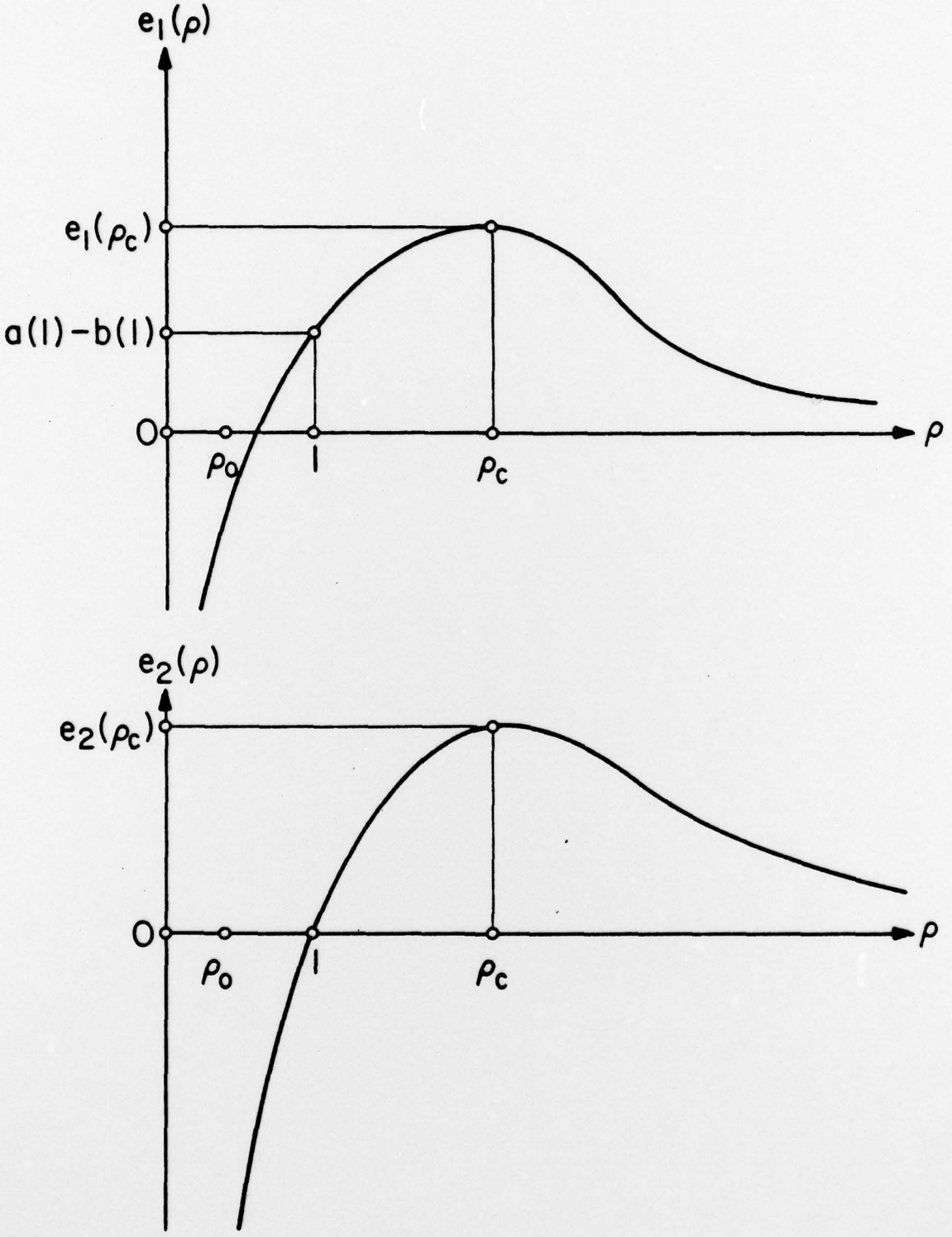

FIGURE 6. QUALITATIVE GRAPHS OF $e_1(\rho)$ AND $e_2(\rho)$.

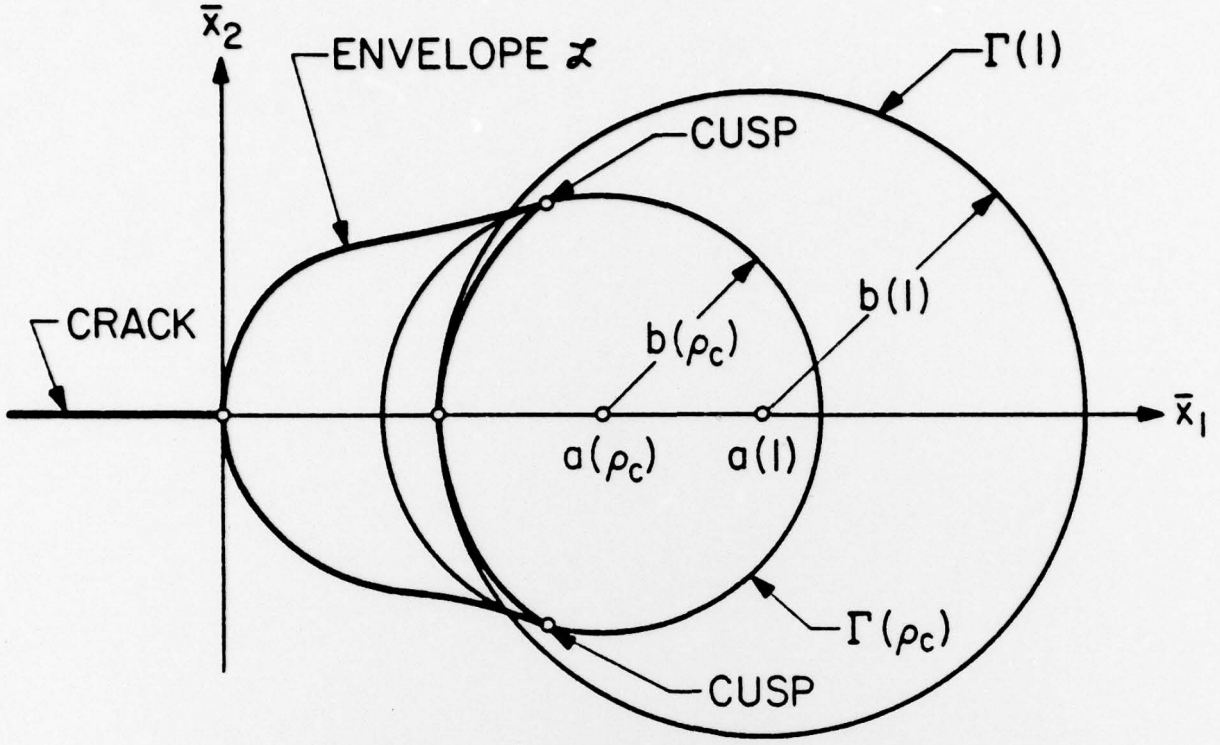

CASE A: $\tau_\infty > 0$

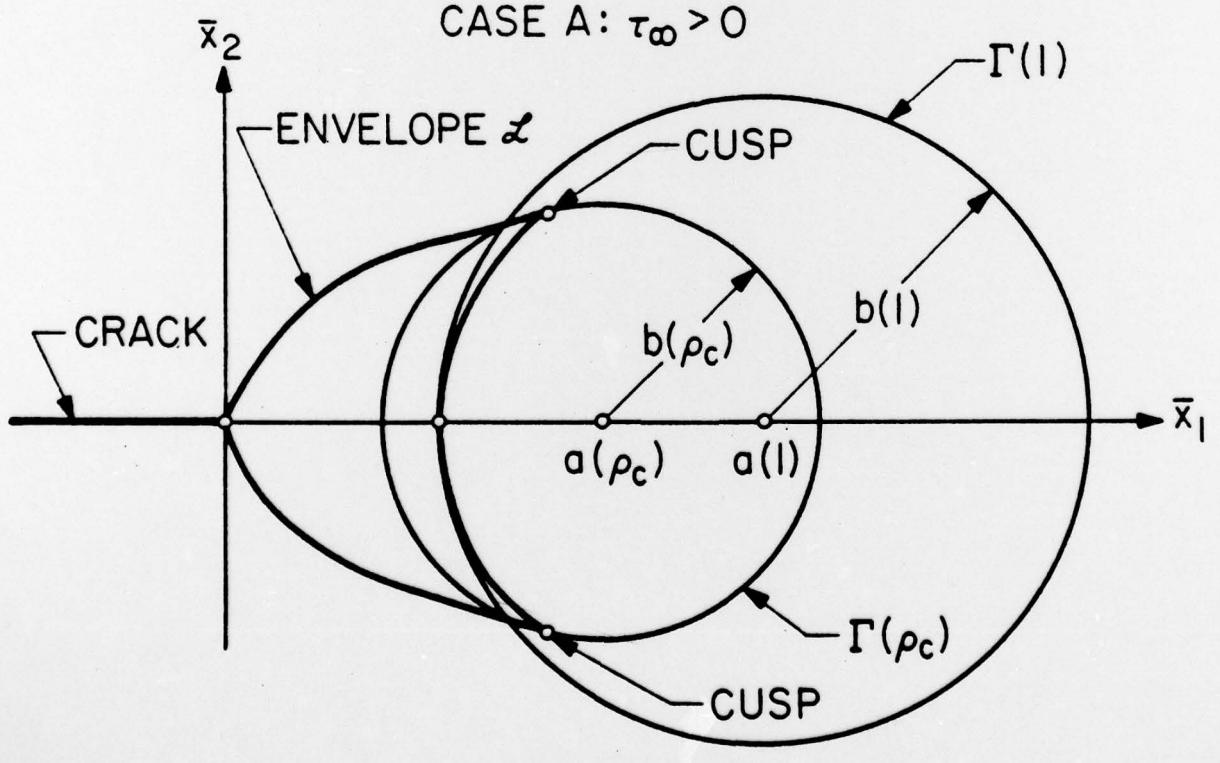

CASE B: $\tau_\infty = 0$

FIGURE 7. ENVELOPE OF CIRCLES $\Gamma(\rho)$ $(1 \leq \rho < \infty)$.

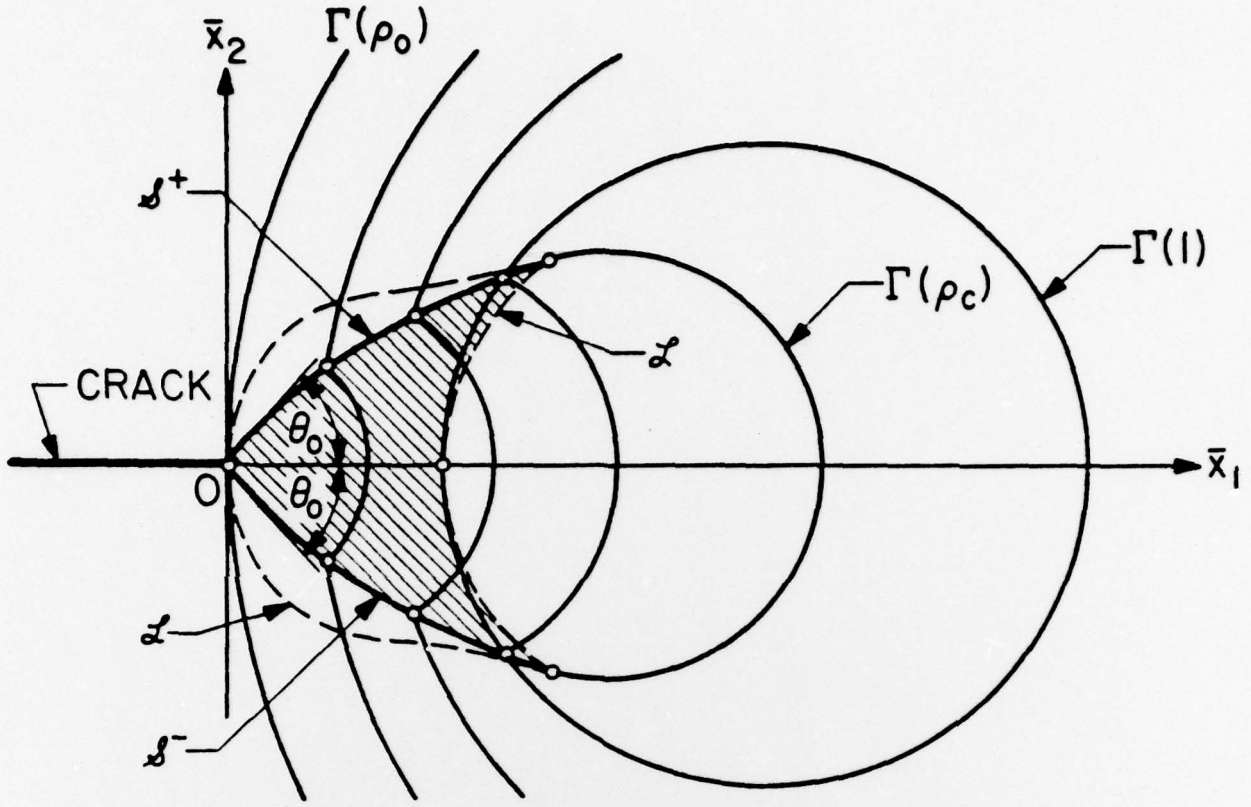

CASE A: $\tau_\infty > 0$

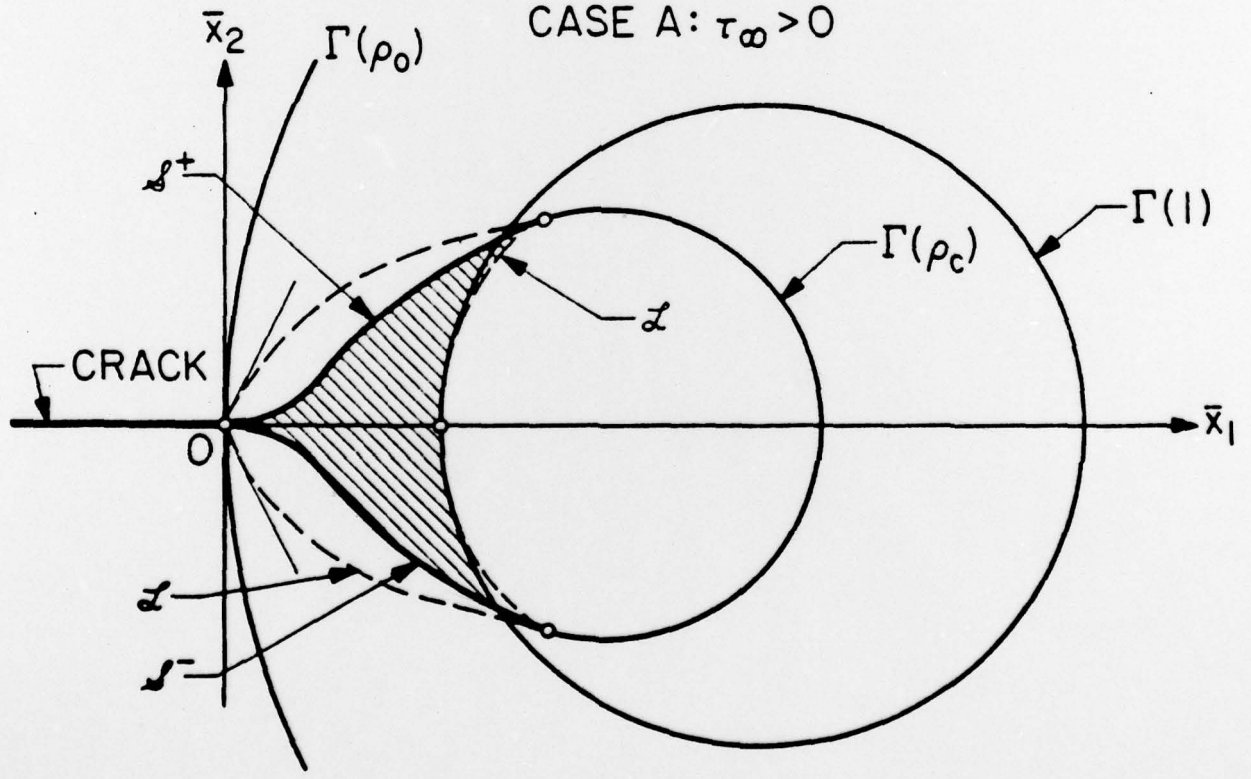

CASE B: $\tau_\infty = 0$

FIGURE 8. SHOCKS $\mathcal{S}^+$, $\mathcal{S}^-$ AND CIRCLES $\Gamma(\rho)$ $(\rho_0 \le \rho < \infty)$.

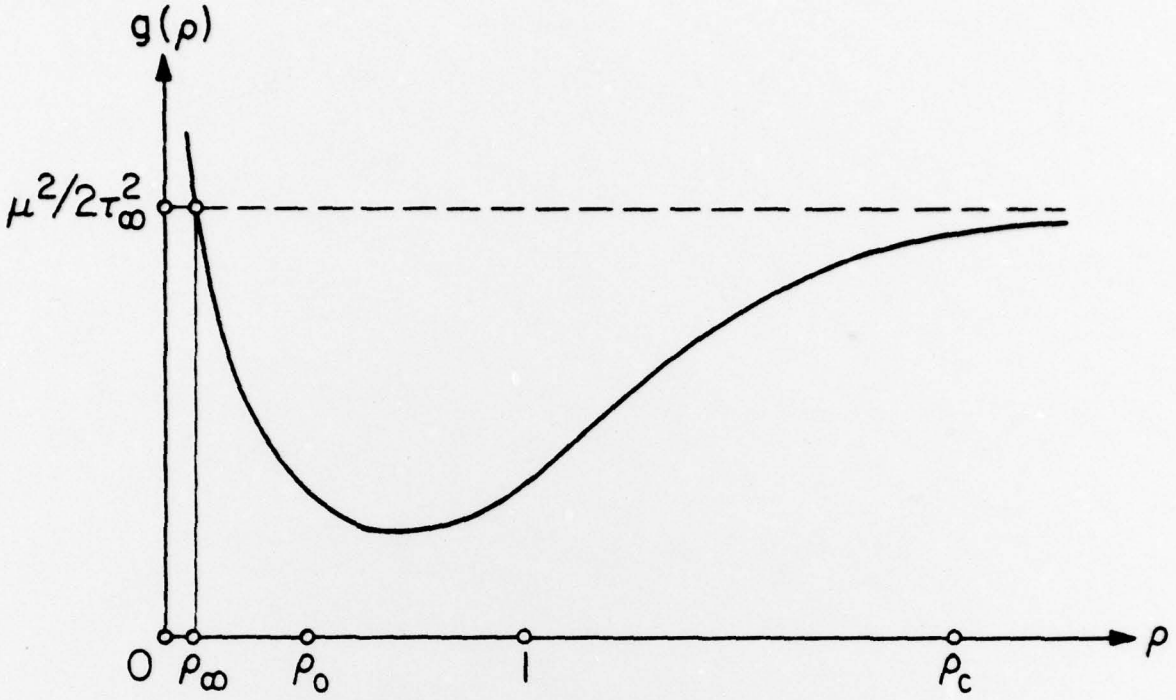

CASE A: $\tau_\infty > 0$

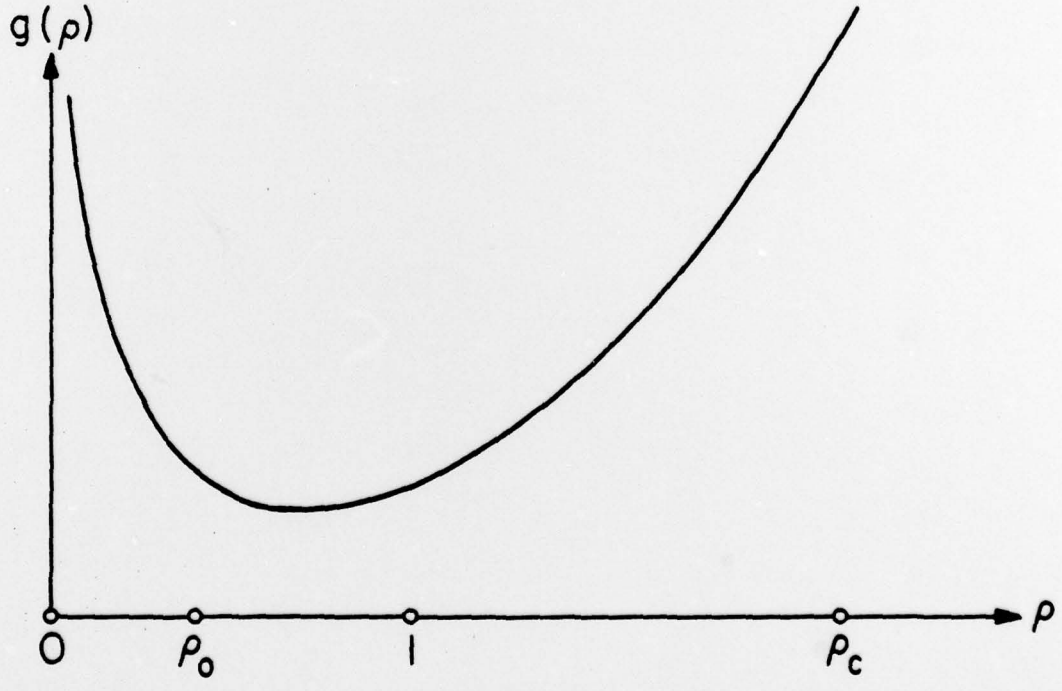

CASE B: $\tau_\infty = 0$

FIGURE 9. QUALITATIVE GRAPH OF $g(\rho)$.

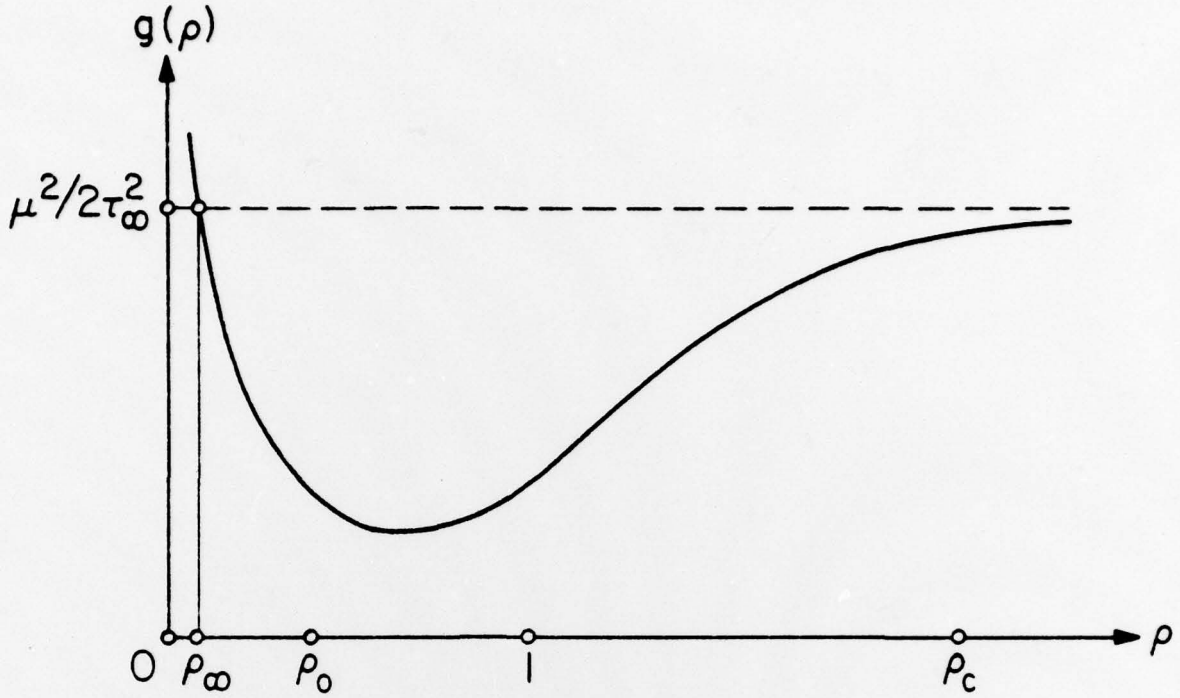

CASE A: $\tau_\infty > 0$

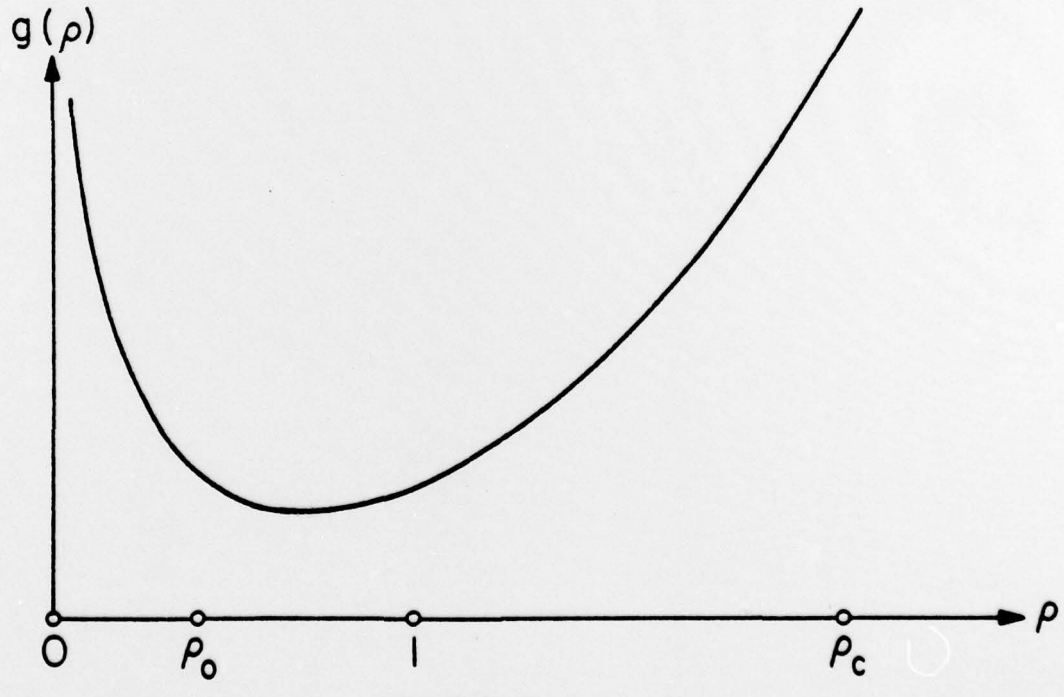

CASE B: $\tau_\infty = 0$

FIGURE 9. QUALITATIVE GRAPH OF $g(\rho)$.

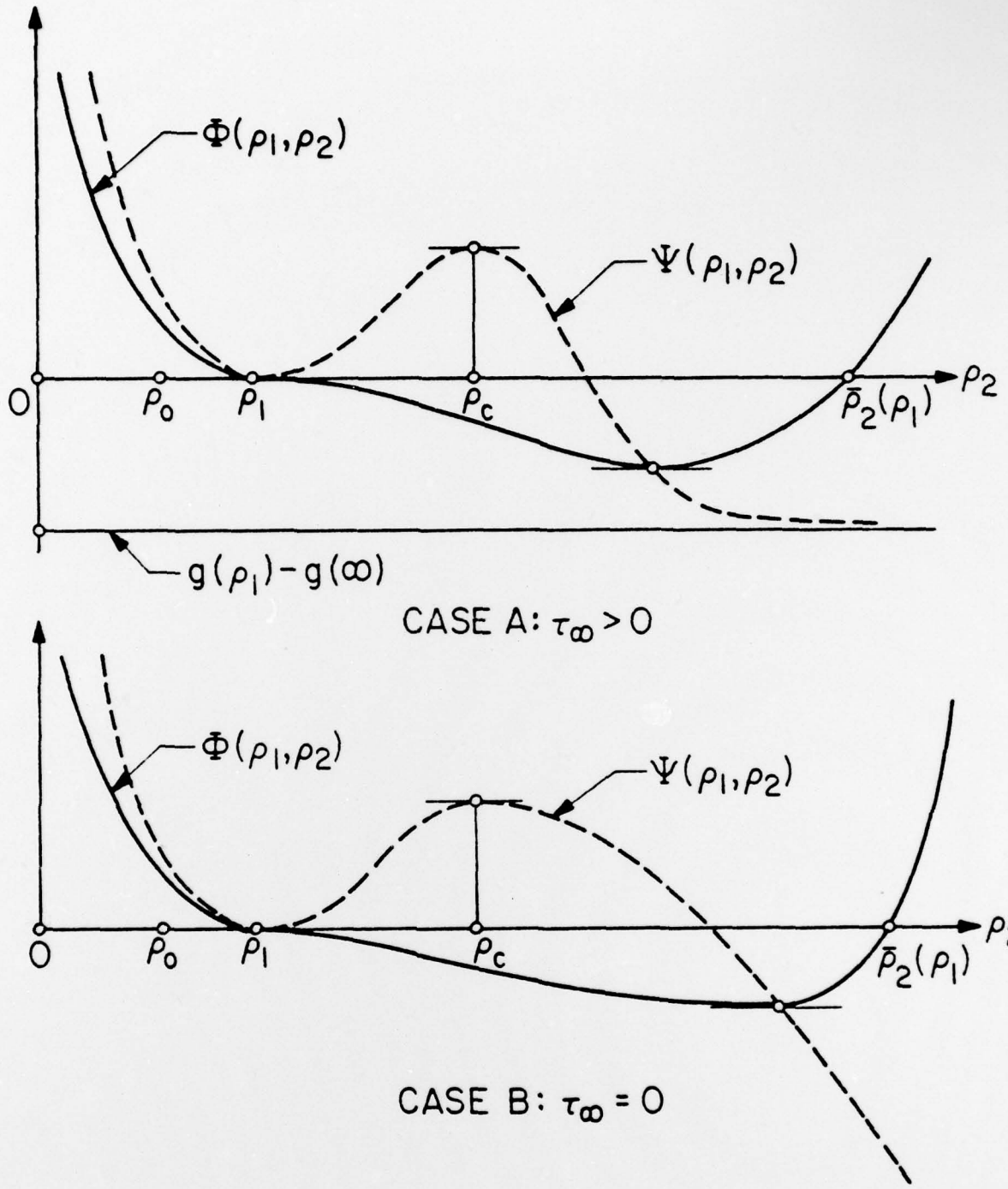

FIGURE 10. QUALITATIVE GRAPHS OF $\Psi(\rho_1, \rho_2)$ AND $\Phi(\rho_1, \rho_2)$ AS FUNCTIONS OF ρ_2 FOR FIXED ρ_1 ($\rho_0 < \rho_1 < \rho_c$).

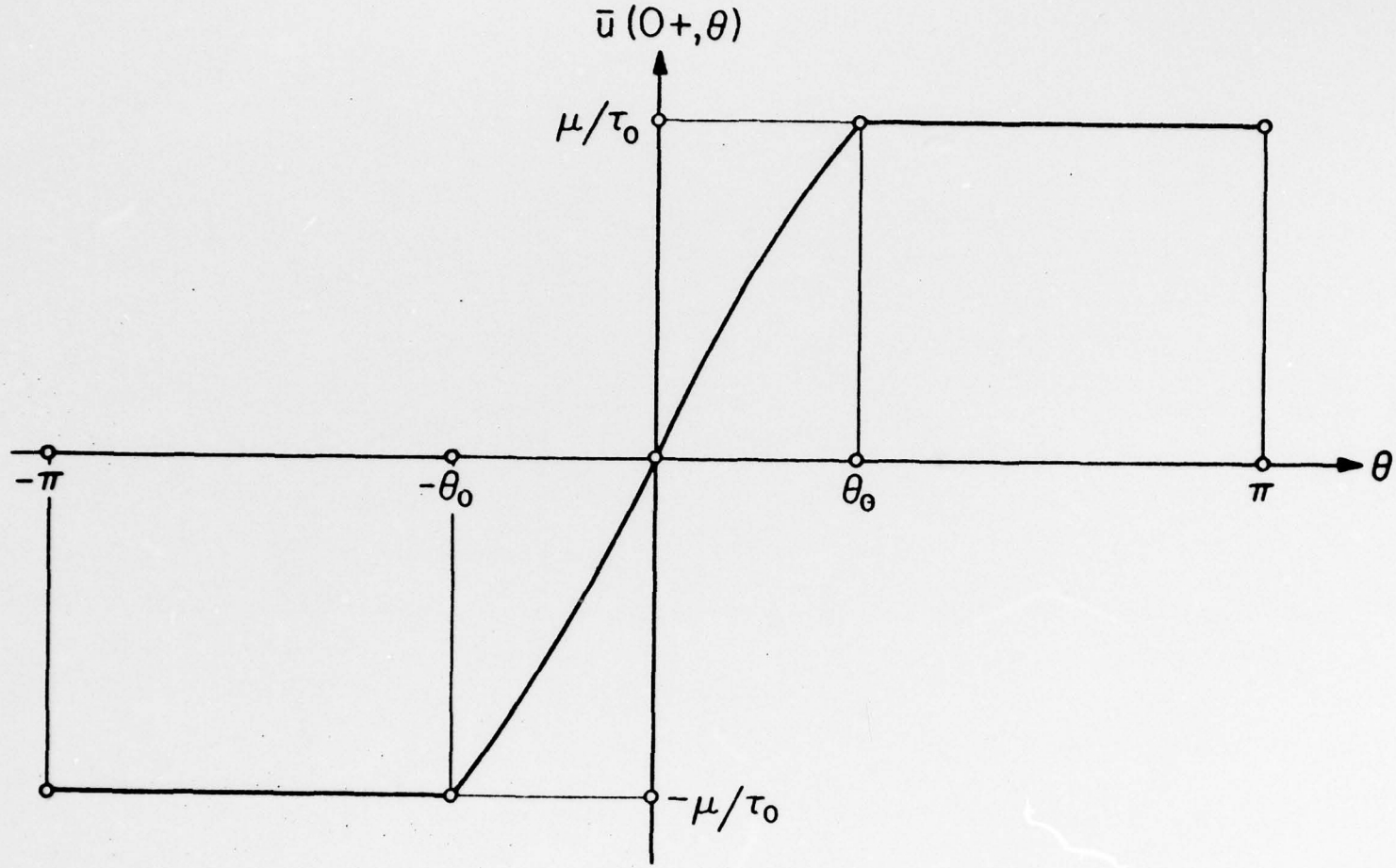

FIGURE II. LIMIT OF $\bar{u}(\bar{r}, \theta)$ AS $\bar{r} \to 0, -\pi \leq \theta \leq \pi, \tau_\infty > 0$.

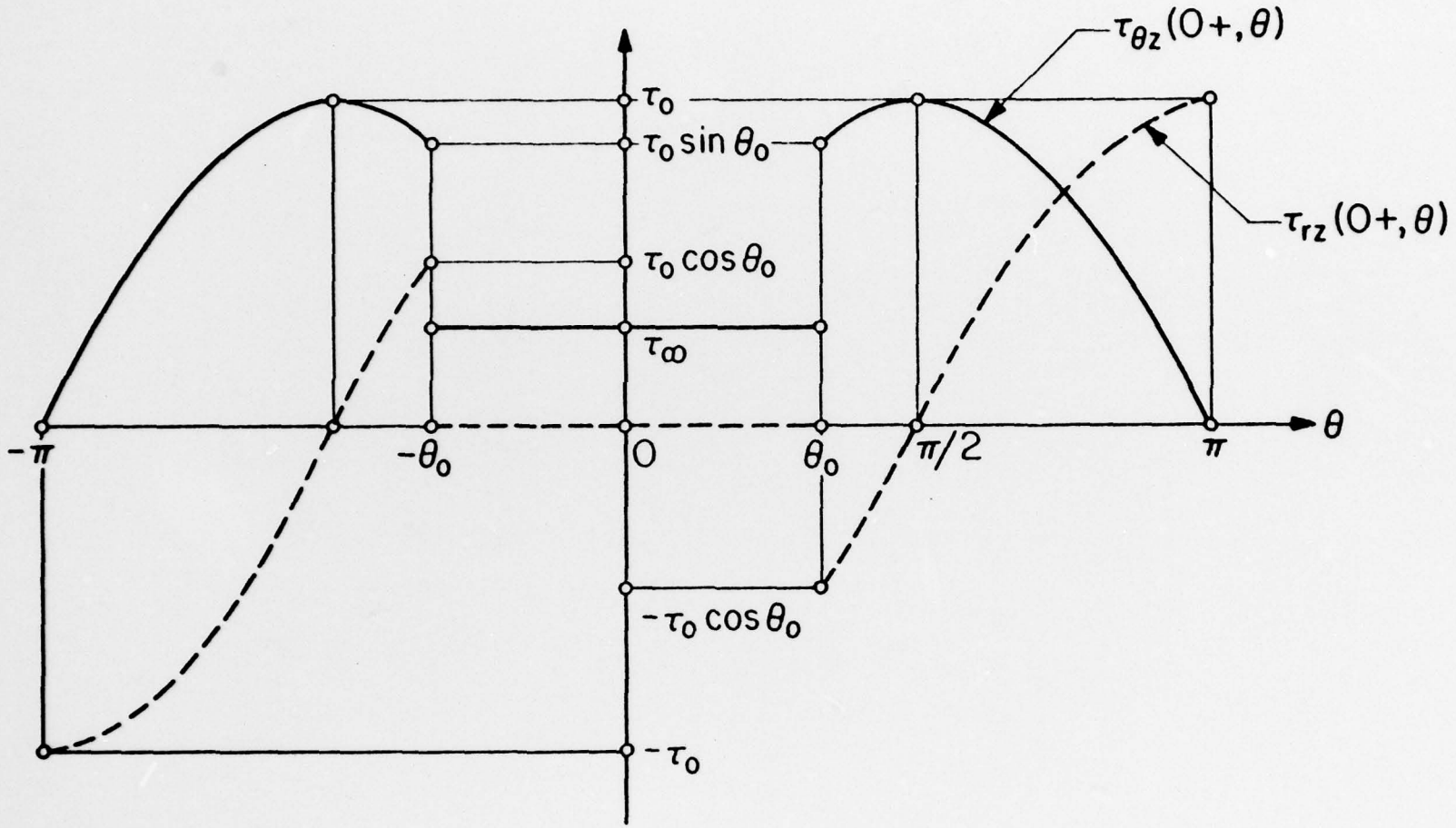

FIGURE 12. LIMIT OF $\tau_{rz}(\bar{r},\theta)$ AND $\tau_{\theta z}(\bar{r},\theta)$ AS $\bar{r} \to 0$, $-\pi \le \theta \le \pi$, $\tau_\infty > 0$.

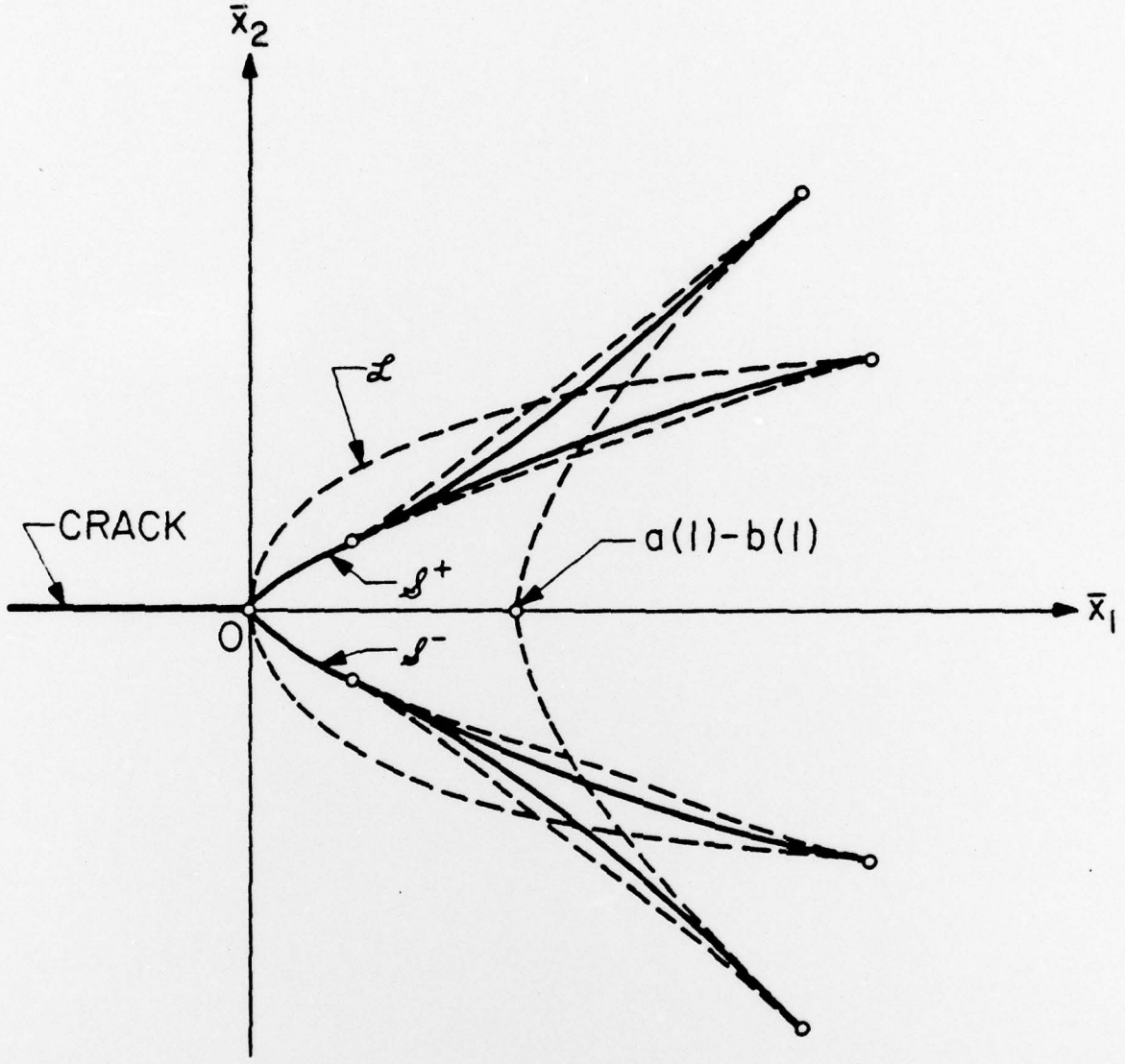

FIGURE 13. A POSSIBLE ENVELOPE $\mathcal{L}$ WITH THREE CUSPS PER BRANCH AND CONJECTURED SHOCKS.

Unclassified

SECURITY CLASSIFICATION OF THIS PAGE (When Data Entered)

REPORT DOCUMENTATION PAGE		READ INSTRUCTIONS BEFORE COMPLETING FORM
1. REPORT NUMBER No. 43	2. GOVT ACCESSION NO.	3. RECIPIENT'S CATALOG NUMBER
4. TITLE (and Subtitle) Anti-plane shear fields with discontinuous deformation gradients near the tip of a crack in finite elastostatics		5. TYPE OF REPORT & PERIOD COVERED Research 6. PERFORMING ORG. REPORT NUMBER
7. AUTHOR(s) J. K. Knowles and Eli Sternberg		8. CONTRACT OR GRANT NUMBER(s) N00014-75-C-0196
9. PERFORMING ORGANIZATION NAME AND ADDRESS California Institute of Technology Pasadena, California 91125		10. PROGRAM ELEMENT, PROJECT, TASK AREA & WORK UNIT NUMBERS
11. CONTROLLING OFFICE NAME AND ADDRESS Office of Naval Research Washington, D. C.		12. REPORT DATE September 1979 13. NUMBER OF PAGES 69
14. MONITORING AGENCY NAME & ADDRESS(if different from Controlling Office)		15. SECURITY CLASS. (of this report) Unclassified 15a. DECLASSIFICATION/DOWNGRADING SCHEDULE

16. DISTRIBUTION STATEMENT (of this Report)

Approved for public release; distribution unlimited

17. DISTRIBUTION STATEMENT (of the abstract entered in Block 20, if different from Report)

18. SUPPLEMENTARY NOTES

19. KEY WORDS (Continue on reverse side if necessary and identify by block number)

Finite elastostatics, cracks, antiplane shear, discontinuous deformation gradients.

20. ABSTRACT (Continue on reverse side if necessary and identify by block number)

This paper reconsiders the problem of determining the elastostatic field near the tip of a crack in an all-around infinite body deformed by a "Mode III" loading at infinity to a state of anti-plane shear. The problem is treated for a class of incompressible, homogeneous, isotropic elastic materials whose constitutive laws permit a loss of ellipticity in the governing displacement equation of equilibrium at sufficiently severe shearing strains. The analysis represents a generalization of that reported in an earlier study and, as before,

DD FORM 1 JAN 73 1473 EDITION OF 1 NOV 65 IS OBSOLETE
S/N 0102-LF-014-6601

Unclassified

SECURITY CLASSIFICATION OF THIS PAGE (When Data Entered)

20. (continued)
is carried out for the "small-scale nonlinear crack problem" in which a crack of finite length is replaced by a semi-infinite one, and the nonlinear field far from the crack-tip is matched to the near field predicted by the linearized theory. The methods employed in the present paper are necessarily largely qualitative, since they apply to all materials in the class considered. The principal feature of the resulting elastic field is the presence of two symmetrically located curves issuing from the crack-tip and bearing discontinuities in displacement gradient and stress.